A MEMRISTIVE CIRCUIT MODEL FOR

P-N JUNCTION DIODES

by

Leon O. Chua and Chong-Wei Tseng

ELECTRONICS RESEARCH LABORATORY

College of Engineering
University of California, Berkeley
94720

A MEMRISTIVE CIRCUIT MODEL FOR P-N JUNCTION DIODES

Leon O. Chua and Chong-Wei Tseng

Department of Electrical Engineering and Computer Sciences
and the Electronics Research Laboratory
University of California, Berkeley, California 94720

ABSTRACT

A new simple lumped circuit model for junction diodes is presented. The model contains only 4 elements; namely, 2 <u>controlled</u> <u>current sources</u>, a <u>nonlinear capacitor</u>, and a <u>memristor</u>. Each component bears a simple relationship with the physical operating mechanisms inside the diode. The model is shown capable of simulating realistically the diode's dynamic behaviors under <u>reverse</u>, <u>forward</u>, and <u>sinusoidal</u> operating modes. Both the <u>storage time</u> and the <u>fall time</u> of the diode can be accurately predicted. The model is also shown capable of mimicking various second order effects due to conductivity modulation. In particular, the model is shown to exhibit a predominantly capacitive incremental impedance under small forward bias and a predominantly inductive impedance under large forward bias. Moreover, it includes the standard two-capacitor model as a special case.

---

i

I. INTRODUCTION

Several circuit models have been proposed for simulating the dynamic behaviors of p-n junction diodes. The simplest model consists of an ideal junction-law diode in parallel with a nonlinear junction capacitance $C_j(v_j)$ and a nonlinear diffusion capacitance $C_d(v_j)$ as shown in Fig. 1(a). We will refer to this circuit as the two-capacitor model [1]. A more general model capable of simulating the diode's conductivity modulation was proposed recently by Barna and Horelick [2] and is shown in Fig. 1(b). But the most sophisticated model capable of providing as accurate an approximation to the diode diffusion equation as possible is Linvill's multi-lumped diffusion model [3] as shown in Fig. 1(c).[1] Linvill's model will simulate the diode diffusion equation exactly as the number of lumped sections approaches infinity. The variables across the nodes in Linvill's model are hole concentrations rather than voltages, and most of the elements used in the model are unconventional ones; namely, combinance H_c, diffusance H_d, and storance S. An equivalent counterpart of Linvill's model using conventional elements such as R's, C's, and controlled sources was recently proposed by Wang and Branin [4] as shown in Fig. 1(d).

Our objective in this paper is to introduce yet another model which possesses the essential features of the above diode models. An important advantage of this new model is its simplicity—it contains only four lumped circuit elements; namely, two controlled sources, a nonlinear capacitor, and a memristor [5]. We will refer to this model as the memristive diode model. In order to compare our model with those

---

[1] For simplicity we assume that it is a single-side (e.g. $N_A \gg N_D$) abrupt-step junction diode.

shown in Fig. 1, however, it is important to point out the basic

dynamic behaviors observed in real junction diodes and the capability

of each model in mimicking these behaviors during reverse and forward

transient operations.

A. Dynamic Behaviors During Reverse Transient

Consider the simple diode circuit shown in Fig. 2(a). Assume that

the switch S is thrown from right to left at $t = t_o$, and that before t_o

the diode is in steady state with a current $i(t) = I_f$, and a voltage

$v(t) = E_f$. Assume $|E_2| >> |E_f|$. Then the reverse transient waveforms

$v(t)$, and $i(t)$ are shown in Fig. 2(b). Observe that there is a small

instantaneous drop in $v(t)$ from E_f to E_o at $t = t_o$. A much larger

instantaneous drop in $i(t)$ from I_f to $-I_r \cong \dfrac{-E_2}{R}$ occurs at $t = t_o$. The

current $i(t)$ remains essentially constant at $-I_r$ until $t = t_o + t_s$ when

the voltage waveform $v(t)$ crosses the time axis. The time interval

t_s is called the storage time. The additional time t_f it takes the

voltage to settle to 90% of the final steady state value is called

the fall time. The storage and fall times represent two important

figures of merit for switching diodes. The storage time t_s depends on

the effective time constant τ as well as the reverse-to-forward

current ratio I_r/I_f.[2] The relationship between the normalized storage

time t_s/τ versus I_r/I_f for long-base diodes as predicted by various

models are shown in Fig. 3. The lowermost curve is the exact solution

of the diode diffusion equation [6]; the corresponding relationships

as predicted by the two-capacitor model and The Linvill's two-lumped

---

[2]It will be shown in section II that for a long base diode, $\tau \cong \tau_p$, the
mean hole recombination life time.

model have been given in [6] and are reproduced here (Fig. 3).[3]

Finally, the relationship predicted by the memristive diode model is also shown in Fig. 3 for comparison purposes. The Linvill and Wang-Branin models give identical relationship since the latter is simply an equivalent representation of the former. The Barna-Horelick model differs from the two-capacitor model only by the additional controlled resistor R_s, which has a negligible effect on t_s; hence the two models also give the same relationship. Observe that these two relationships differ significantly from the ideal one (the lowermost curve in Fig. 3), while that predicted by the memristive diode model to be presented in Section II represents a much better approximation. Of course, by increasing the number of lumped sections in Linvill's model, it is possible to approach the ideal curve. However, from the computer circuit simulation point of view, the memristive diode model is much more economical since it requires only four elements.

The fall time t_f depends on how fast the residual stored charge can be discharged. Both the two-capacitor and the Barna-Horelick model have predicted fall times which are typically three order of magnitude smaller than actually observed [4]. Consequently, they are unsatisfactory for analyzing many high speed circuits, such as switching circuits. The Linvill and Wang-Branin model could predict a much more accurate t_f so long as a sufficient number of lumped sections are chosen. A typical

---

[3]Actually the uppermost relationship shown in Fig. 3 is the solution of the equation $-I_r = \dfrac{dq'_p}{dt} + \dfrac{q'_p}{\tau_p}$, where q'_p is the charge of excess carriers stored in base, I_r is the magnitude of the initial reverse current. But this equation is precisely the governing equation for the two-capacitor model during reverse transient. See Appendix A.

number required for accurate prediction has been reported to be 20 sections [4]. Such model is often too complicated for simulating circuits containing many diodes. In contrast to this, it will be shown in Section III that the memristive diode model is capable of approximating an accurate t_f by only adjusting one of the model parameters.

B. Dynamic Behaviors During Forward Transient

Consider the diode circuit shown in Fig. 4(a) where a positive step current $i_s(t)$ as shown in Fig. 4(b) is applied at $t = 0$ when the diode is in zero state. The associated diode voltage waveform $v(t)$ for $t \geq 0$ is shown in Fig. 4(b) corresponding to three different values of current amplitudes I_f. It is well known that for small current amplitudes, the voltage $v(t)$ increases monotonically to its steady state value [7]. Conversely, for large current amplitudes, the voltage $v(t)$, after an initial overshoot, decreases monotonically to its steady state value. In between, there exists a range of intermediate current amplitudes where $v(t)$ has an oscillatory component which decays quickly to zero. The above three distinct forward transient behaviors are depicted in Fig. 4(b).

Another general dynamic characteristic of junction diode under forward bias is that its small-signal sinusoidal response varies from a prediominantly capacitive impedance under low forward bias to a predominantly inductive impedance under high forward bias. In between, a ringing phenomenon is observed [7-10].

The above forward transient behaviors are due mainly to the conductivity modulation arising from the variation of stored charge as a

function of the external excitation and the internal state of the diode. Among the four models shown in Fig. 1, only the Barna-Horelick model is capable of simulating the forward transient behaviors accurately. This is achieved through the introduction of a linear resistance R_s whose value is controlled by the junction current $i_j(t)$, which in turn is a function of the junction voltage $v_j(t)$. Observe that as the capacitors C_d and C_j are charged or discharged, R_s decreases or increases, thereby providing a mechanism for simulating the conductivity modulation. However, it is a poor model for simulating reverse transient behaviors as we have already indicated earlier. In contrast to this, the memristive diode model will be shown capable of predicting both forward and reverse transient behaviors. Here the memristor will be seen to play a crucial role in mimicking the charge storage effect in the diode base.

II. THE MEMRISTIVE DIODE MODEL

Consider the one dimensional p-n junction diode shown in Fig. 5(a) with an n-type region of width W_n and junction area A. Assume that the p-type region is much more heavily dopped than the n-type region. Hence, the hole current at the junction is approximately equal to the total diode current. The memristive diode model as derived from the physical operating mechanism of the diode is shown in Fig. 5(b). The four circuit elements in this model are characterized as follows:

(1) <u>The nonlinear junction capacitance</u> [4].

---

[4] Equations (1) and (2) are the depletion approximation for a single-side abrupt-step junction diode. For a linearly-graded junction diode, the exponent 1/2 and the constant K_a must be modified accordingly [6].

$$C_j(v_j) = \frac{K_a}{2}(\psi_o - v_j)^{-\frac{1}{2}} \qquad (1)$$

$$K_a \triangleq A[2\varepsilon q\, N_D]^{\frac{1}{2}} \qquad (2)$$

where

ψ_o = built-in voltage

ε = dielectric permitivity of the semiconductor

q = magnitude of electron charge

N_D = donor concentration in the n-type region.

(2) The memristor[5]

$$R_m(q_m) = \frac{1}{A}\int_0^{W_n}\frac{dx}{\sigma(x,q_m)} \qquad (3)$$

$$\sigma(x,q_m) = q\mu_n n_{no} + q\mu_p\left\{P_{no} + \frac{q_m}{AqL_p}\left(\frac{\sinh\left(\frac{W_n}{L_p}\right)}{\cosh\left(\frac{W_n}{L_p}\right)-1}\right)\left[\cosh\left(\frac{x}{L_p}\right) - \coth\left(\frac{W_n}{L_p}\right)\right.\right.$$
$$\left.\left. \sinh\left(\frac{x}{L_p}\right)\right]\right\} \qquad (4)$$

where[6]

μ_n = electron mobility

μ_p = hole mobility

_____

[5]The memristor is a two-terminal circuit element defined by $v_m = R_m(q_m)\, i_m$, where $R_m(q_m)$ is a <u>linear</u> resistance whose value depends on the charge q_m passing through its terminals [5]. A memristor can be considered therefore as a charge-controlled linear resistor.

[6]Equation (4) is valid only in the low injection case where electrons can be considered as the majority carriers. For our purpose, however, Eq. (4) is adequate.

n_{no} = equilibrium electron concentration in n-type region

P_{no} = equilibrium hole concentration in n-type region

A = junction area of the diode

W_n = width of the n-type region (base width)

$L_p = \sqrt{D_p \tau_p}$ = hole diffusion length

D_p = hole diffusion constant

τ_p = hole recombination life time

(3) The controlled current source $i_2 = I_2(q_m)$

$$I_2(q_m) = \frac{q_m}{\tau} \tag{5}$$

$$\tau \triangleq \tau_p \left[1 - \text{sech}\left(\frac{W_n}{L_p} \right) \right] \tag{6}$$

where τ_p, w_n, and L_p are as defined above. We call τ the _effective hole life time_. Since sech $x \leq 1$ for all x, we have $0 \leq \tau \leq \tau_p$. Observe that $\tau \to 0$ as $W_n \to 0$ and $\tau \to \tau_p$ as $W_n \to \infty$. For long base diodes with $W_n \gg L_p$, we have $\tau \approx \tau_p$.

(4) The controlled current source $i_1 = I_1(i, i_j, v_j, q_m)$

$$I_1(i, i_j, v_j, q_m) = I_{1f} U(i) + I_{1r} U(-i) \tag{7}$$

where U(·) is the unit step function[7], and

_____

[7]The unit step function is defined by $U(x) = \begin{cases} 1, & x > 0 \\ \frac{1}{2}, & x = 0 \\ 0, & x < 0 \end{cases}$

If the discontinuity at x = 0 is objectionable, U(x) can be replaced by its continuous approximation U(x,K,δ) as in appendix B.

$$I_{1f} \overset{\Delta}{=} I_s \left[\exp\left(\frac{v_j}{V_T}\right) - 1 \right] + \frac{C_d(v_j)}{C_j(v_j)} \, i_j \tag{8}$$

where I_s = diode saturation current

$$V_T = \frac{kT}{q} = \text{thermal voltage}$$

$$C_d(v_j) \overset{\Delta}{=} \frac{I_s \tau}{V_T} \, \exp\left(\frac{v_j}{V_T}\right) \tag{9}$$

is the diode diffusion capacitance, and $C_j(v_j)$ is as defined in (1). The quantity I_{1r} is defined by:[8]

$$I_{1r} \overset{\Delta}{=} i - C_j(v_j) \max(\gamma_a, \gamma_b) \tag{10}$$

where

$$\gamma_a \overset{\Delta}{=} \frac{i}{C_j(v_j) \left\{ 1 + \alpha \left[\dfrac{|q_m| + I_s \tau}{(|i| + I_s)\,\tau} \right] U(-v_j) \right\}} \tag{11}$$

$$\gamma_b \overset{\Delta}{=} -\max(\gamma_c, \gamma_d) \tag{12}$$

$$\gamma_c \overset{\Delta}{=} \frac{I_s \left[\exp\left(\dfrac{v_j}{V_T}\right) - 1 \right] - i}{C_d(v_j) + C_j(v_j)} \tag{13}$$

---

[8] The function max ($\cdot$, $\cdot$) is defined by
          max (x,y) = x whenever x $\geq$ y
                    = y whenever x < y.
If necessary, max (x,y) can be replaced by a differentiable function M(x,y,K,δ) as defined in appendix C.

and

$$\gamma_d \triangleq \frac{\left\{ \dfrac{V_T \sinh\left(\dfrac{W_n}{L_p}\right)}{AqL_p\left[\cosh\left(\dfrac{W_n}{L_p}\right) - 1\right]} \right\} q_m}{P_{no}\left\{1 + \exp\left(\dfrac{v_j}{[1-0.5v_j\, U(-v_j)]\, V_T}\right)\right\}\left\{0.25\tau\left[\dfrac{|q_m| + I_s\tau}{(|i| + I_s)\tau}\right]^\beta\right\}} \tag{14}$$

The physical parameters I_s, τ, V_T, A, q, W_n, and L_p in

Eqs. (11) − (14) are as defined above, while "α" and "β" are <u>empirical</u>

parameters whose value can be chosen to obtain an accurate prediction

for the storage time t_s as well as the fall time t_f. Typically, $\beta = 1.5$,

and $0.5 \leq \alpha \leq 10$. The precise value of α depends on how much the residual

stored charge still remains in the base region of a particular diode

at $t = t_o + t_s$ and on how fast it can be discharged.

Observe that the memristive diode model is specified by 13

physical diode parameters $\{\psi_o, \epsilon, N_D, \mu_n, \mu_p, n_{no}, P_{no}, A, W_n, D_p, \tau_p,$

$V_T, I_s\}$ and two empirical diode parameters $\{\alpha, \beta\}$. Among the 13 physical

parameters, several are constrained by well-known relationships.

Moreover, typical values of most of these parameters are known and

precise values for a particular diode can be obtained through standard

computer optimization techniques [11].

The capability of the memristive diode model will be discussed in

detail in Section IV with numerical examples. However, in order to

understand why and how this model works, we now turn to Section III

and show how this model is derived from the physical operating principles

of the diode. The few occasions where an empirical term is introduced

will also be pointed out along with the reason for its introduction.

III. DERIVATION OF THE MODEL

Consider the one-dimensional diode shown in Fig. 5(a) under the assumptions enunciated in Section II (i.e. $N_A \gg N_D$, and assuming an abrupt-step junction). We know from diode physics that there exists a thin transition layer at the junction, and that the resistance in the neutral region depends solely on the carriers available there. Observe that as carriers flow through a diode, they either flow into the transition layer and change the amount of charge stored there, or leak through the layer into the neutral regions[9] where they are recombined or stored. In the latter case, the carrier concentration in the neutral regions may change, thereby inducing a corresponding change in the conductance. These basic diode operating mechanisms are incorporated in the model shown in Fig. 5(b) where C_j is used to represent the effect of the transition layer, i_1 is used to simulate the leakage of carriers through the layer, R_m is used to simulate the conductance of the neutral regions, and i_2 is used to represent the recombination of carriers. The characterizing functions for these four elements are also derived from basic physical principles:

(1) The nonlinear junction capacitance $C_j(v_j)$.

For simplicity we choose the standard expression for $C_j(v_j)$ as derived from the depletion approximation for a one-dimensional diode with an abrupt-step and single-side (i.e., $N_A \gg N_D$) junction [6]. This expression is given by Eqs. (1) and (2).

---

[9]These two distinct mechanisms actually operate simultaneously.

(2) The memristor $R_m(q_m)$.

Since $N_A \gg N_D$, the conductance of p-type region is much greater than that of the n-type region, i.e., the resistance of the diode is mainly contributed by the n-type region (the base region). The conductivity $\sigma(x)$ of the base region under low injection condition is

$$\sigma(x) = q\{\mu_n \, n_{no} + \mu_p \, p_n(x)\} \qquad (15)$$

where $p_n(x)$ is the hole concentration at x, (x is measured from the junction into the base region). In order to evaluate $p_n(x)$, let us consider the one dimensional diode <u>steady state</u> diffusion equation [6]

$$\frac{\partial^2 p_n'(x)}{\partial x^2} - \frac{p_n'(x)}{L_p^2} = 0 \qquad (16)$$

where $p_n'(x) \overset{\Delta}{=} p_n(x) - p_{no}$ is the excess hole concentration at x in the base region.

The boundary conditions are:

(a) at x = 0:

$$p_n'(x) = p_n'(0) = p_{no} \left[\exp\left(\frac{v_j}{V_T}\right) - 1 \right] \qquad (17)$$

where v_j is the applied voltage across the diode junction.

(b) at $x = W_n$:

$$S_p \times p_n'(W_n) = \frac{1}{q} J_p(W_n) = - D_p \left. \frac{\partial p_n'(x)}{\partial x} \right|_{x = W_n} \qquad (18)$$

-12-

where S_p is the surface recombination velocity [6], and $J_p(x)$ the hole current density at x.

The solution of Eq. (16) subject to Eqs. (17) and (18) is:

$$p_n'(x) = p_n'(0) \left[\cosh\left(\frac{x}{L_p}\right) - \left(\frac{\cosh\left(\frac{W_n}{L_p}\right) + \frac{D_p}{L_p S_p} \sinh\left(\frac{W_n}{L_p}\right)}{\frac{D_p}{L_p S_p} \cosh\left(\frac{W_n}{L_p}\right) + \sinh\left(\frac{W_n}{L_p}\right)} \right) \sinh\left(\frac{x}{L_p}\right) \right] \quad (19)$$

If S_p is very large,[10] then

$$p_n'(x) = p_n'(0) \left[\cosh\left(\frac{x}{L_p}\right) - \coth\left(\frac{W_n}{L_p}\right) \sinh\left(\frac{x}{L_p}\right) \right] \quad (20)$$

The stored excess minority charge q_p' is

$$q_p' = \int_0^{W_n} Aq\, p_n'(x)\, dx = Aq\, p_n'(0)\, L_p \left[\frac{\cosh\left(\frac{W_n}{L_p}\right) - 1}{\sinh\left(\frac{W_n}{L_p}\right)} \right] \quad (21)$$

solving for $p_n'(0)$ from Eq. (21) and substituting it into Eq. (20), we obtain:

$$p_n'(x) = \frac{q_p'}{AqL_p} \left(\frac{\sinh\left(\frac{W_n}{L_p}\right)}{\cosh\left(\frac{W_n}{L_p}\right) - 1} \right) \left[\cosh\left(\frac{x}{L_p}\right) - \coth\left(\frac{W_n}{L_p}\right) \sinh\left(\frac{x}{L_p}\right) \right] \quad (22)$$

---

[10]This standing assumption is satisfied when the base terminal contact has plenty of electrons and/or recombination centers to recombine any excess hole there.

Replacing q_p' in Eq. (22) by q_m[11], and substituting the resulting

expression into Eq. (15), we obtain Eq. (4) (where we have also made

use of $p_n(x) = p_{no} + p_n'(x)$). The resistance in the base region is

given by $R_m(q_m) = \displaystyle\int_0^{W_n} \frac{dx}{A\,\sigma(x,q_m)}$, which is Eq. (3). A typical curve for

R_m as a function of q_m is shown in Fig. 6.

(3) The controlled current source $i_2 = I_2(q_m)$.

From Eq. (21),

$$q_p' = Aq\,p_n'(0)\,L_p \left[\frac{\cosh\left(\dfrac{W_n}{L_p}\right) - 1}{\sinh\left(\dfrac{W_n}{L_p}\right)} \right]$$

$$= \left[\frac{Aq\,D_p\,p_n'(0)}{L_p}\, \coth\left(\frac{W_n}{L_p}\right) \right] \left\{ \left[1 - \operatorname{sech}\left(\frac{W_n}{L_p}\right) \right] \tau_p \right\} \qquad (23)$$

where we have used the identity $L_p^2 = D_p\,\tau_p$.

On the other hand the diode current is given by:

$$i \approx A\,J_p(0) = -Aq\,D_p\, \left. \frac{\partial\,p_n'(x)}{\partial x} \right|_{x=0} \qquad (24)$$

It follows from Eqs. (20) and (24) that

$$i = \frac{Aq\,D_p\,p_n'(0)}{L_p}\, \coth\left(\frac{W_n}{L_p}\right) \qquad (25)$$

---

[11]The replacement of q_p' by the memristor charge q_m will be justified soon.

Equations (23) and (25) together give

$$q_p' = i \tau \tag{26}$$

where τ is the _effective_ hole life time defined in Eq. (6). If follows from Eq. (26) that a hole, on the average, stays in the base τ seconds before it is recombined or passes through the base.

If we define i_2 as

$$i_2 = q_m/\tau \tag{27}$$

then at steady state, i.e., when $\dot{q}_m = 0$ and consequently no current flows through the memristor, we have $i = i_2$ and

$$\frac{q_p'}{\tau} = \frac{q_m}{\tau} \tag{28}$$

This constraint justifies the identification of q_p' with q_m. It follows from Eqs. (26) and (27) that at steady state, the diode current i must feed the bulk recombination in the base at a recombination rate of q_p'/τ [6]. The introduction of the controlled current source $i_2 = q_m/\tau$ is therefore necessary for simulating this mechanism.

(4) The controlled current source $i_1 = I_1(i, i_j, v_j, q_m)$.

To derive Eq. (7) for i_1 let us rewrite it as follows:

$$i_1 = \begin{cases} i_{1f}, & \text{when } i > 0 \\ i_{1r}, & \text{when } i < 0 \end{cases}$$

Clearly, i_{1f} should be defined in such a way that the resulting model will mimic the essential features of the diode static and dynamic characteristics when $i > 0$ (including forward transient behaviors). A similar requirement applies to the definition of I_{1r}. Now, if we define I_{1f} as in Eq. (8), we can recast it into the following form:

$$I_{1f} = I_s \left[\exp\left(\frac{v_j}{V_T}\right) - 1 \right] + C_d(v_j) \left[\frac{i_j}{C_j(v_j)} \right]$$

$$= I_s \left[\exp\left(\frac{v_j}{V_T}\right) - 1 \right] + C_d(v_j) \frac{dv_j}{dt}$$

(29)

Equation (29) can be interpreted as the governing equation for a circuit consisting of an ideal junction-law diode in parallel with a nonlinear capacitor with capacitance $C_d(v_j)$ as defined in Eq. (9), which is the conventional expression for the diode diffusion capacitance. Hence, when $i > 0$, the upper part of the hinged circuit in Fig. 5(b) is equivalent to the two-capacitor model. It is now clear that the lower portion of the memristive diode model is responsible for simulating those forward transient behaviors found wanting in the two-capacitor model, the Linvill model, and the Wang-Branin model.

To derive I_{1r}, consider again the circuit shown in Fig. 2(a). It is well known that the carrier concentration distribution after $t = t_o$ is as shown in Fig. 7, where the concentration gradient at $x = 0$ is proportional to the diode current, and where the carrier concentration at $x = 0$ reaches the equilibrium value p_{no} at $t = t_o + t_s$ [12]. For a long base diode, t_s/τ and I_r/I_f are related as follows [13]:

$$
\text{erf} \left[(t_s/\tau)^{1/2} \right] = \frac{1}{1 + I_r/I_f} \tag{30}
$$

where erf($\cdot$) denotes the error function. To incorporate the above observations into our model, we note that at <u>steady state</u> $p_n'(0)$, the excess carrier concentration at $x = 0$, is related to the stored charge q_p' (or q_m) by Eq. (21). To emphasize that Eq. (21) is valid only at steady state, we denote the steady state excess carrier concentration by $\bar{p}_n'(0)$, and the steady state stored charge by $\bar{q}_m$ and recast Eq. (21) as follows:

$$
\bar{p}_n'(0) = \frac{\bar{q}_m}{AqL_p} \left[\frac{\sinh\left(\frac{W_n}{L_p}\right)}{\cosh\left(\frac{W_n}{L_p}\right) - 1} \right] \tag{31a}
$$

Let us now define a quantity $\bar{p}_n'(0,t)$ as follows:

$$
\bar{p}_n'(0,t) = \frac{q_m(t)}{AqL_p} \left[\frac{\sinh\left(\frac{W_n}{L_p}\right)}{\cosh\left(\frac{W_n}{L_p}\right) - 1} \right] \tag{31b}
$$

Observe that Eq. (31b) reduces to Eq. (31a) in steady state. Next, we <u>postulate</u> the following constraint on the rate of change of the excess carrier concentration $p_n'(x)$ at $x = 0$:[12]

---

[12] The terms $I_s\tau$ and I_s in Eq. (32) are very small constants which are introduced to avoid computer overflow problem when $q_m(t) = 0$, or $i(t) = 0$.

$$\frac{d\, p_n'(0)}{dt} = - \frac{\bar{p}_n'(0,t)}{\left[0.25\tau \ \frac{|q_m(t)| + I_s\tau}{(i(t) + I_s)\,\tau}\right]^\beta} \tag{32}$$

To justify the reason for introducing this constraint, we observe that if $\beta = 1$, and if the initial reverse current $-i(t_o) = I_r$ is equal to $q_m(t_o)/\tau = I_f$, then since $i(t) \approx i(t_o)$ for $t \leq t_o + t_s$, we have

$$\frac{d\, p_n'(0)}{dt} = - \frac{\bar{p}_n'(0,t)}{0.25\tau\left[\frac{|q_m(t)| + I_s\tau}{(|i(t_o)| + I_s)\,\tau}\right]} \approx - \frac{\frac{q_m(t)}{AqL_p}\left[\frac{\sinh\left(\frac{W_n}{L_p}\right)}{\cosh\left(\frac{W_n}{L_p}\right) - 1}\right]}{0.25\tau\left[\frac{q_m(t)}{|i(t_o)|\tau}\right]}$$

$$= - \frac{\frac{|i(t_o)|}{AqL_p}\left[\frac{\sinh\left(\frac{W_n}{L_p}\right)}{\cosh\left(\frac{W_n}{L_p}\right) - 1}\right]}{0.25} = - \frac{\frac{q_m(t_o)}{AqL_p}\left[\frac{\sinh\left(\frac{W_n}{L_p}\right)}{\cosh\left(\frac{W_n}{L_p}\right) - 1}\right]}{0.25\tau}$$

$$= - \frac{\bar{p}_n'(0,t_o)}{0.25\tau} = \text{constant} \tag{33}$$

Equation (33) implies that if we switch a diode with a reverse current whose magnitude I_r is equal to the forward steady state current I_f, then $p_n'(0)$ will become zero at $t = t_o + 0.25\ \tau$. This observation is consistent with that predicted by Eq. (30); namely, if $I_r \approx I_f$, then $t_s \approx 0.25\ \tau$, i.e., $v_j(t_s) = v_j(0.25\tau) = 0$.

Since

$$p_n'(0) = p_{no}\left[\exp\left(\frac{v_j}{v_T}\right) - 1\right] \tag{34}$$

$p_n'(0)$ also becomes zero at $t = t_o + 0.25 \ \tau$. Thus we see Eq. (32) indeed represents a "qualitatively" reasonable constraint. It follows from Eqs. (32) and (34) that

$$- \frac{d \ v_j}{dt} = \frac{V_T \ \bar{p}_n'(0,t)}{P_{no} \ \exp\left(\frac{v_j}{V_T}\right) 0.25\tau \left[\frac{|q_m(t)| + I_s \ \tau}{(|i(t)| + I_s)\tau}\right]^\beta} \tag{35}$$

If we use only Eq. (35) to calculate $v_j(t)$ and t_s during reverse transient, two problems immediately arise:

(i) It predicts too long a storage time t_s when $I_r << I_f$.

(ii) When $t > t_o + t_s$, $v_j(t) < 0$ and $\exp\left(\frac{v_j}{V_T}\right) \approx 0$. Hence, $\left|\frac{dv_j}{dt}\right|$ becomes exceedingly large, thereby resulting in "too short" a fall time t_f, let alone the computer over flow problem that invariably arises. To overcome these problems, we first modify Eq. (35) as follows:[13]

$$- \frac{dv_j}{dt} = \frac{V_T \ \bar{p}_n'(0,t)}{P_{no} \left\{1 + \exp\left(\frac{v_j}{[1-0.5 \ v_j \ U(-v_j)] \ V_T}\right)\right\} \left\{0.25\tau \left[\frac{|q_m(t)| + I_s\tau}{(|i(t)| + I_s)\tau}\right]^\beta\right\}} \tag{36}$$

Observe that Eq. (36) is equivalent to Eq. (35) when $v_j >> V_T$. However, when $v_j < 0$ there is no overflow problem since

---

[13]This modification will differ significantly from Eq. (35) only when $v_j < 0$. However, in this case the discrepancy is immaterial because, as will be shown later, when $v_j < 0$, the model will automatically replace Eq. (35) with a more realistic expression; namely, $\frac{dv_j}{dt} = \gamma_a$, where γ_a is defined in Eq. (11).

$$\exp\left(\frac{v_j}{[1-0.5\ v_j\ U(-v_j)]\ V_T}\right) \rightarrow \exp(-2/V_T),\ \text{as}\ v_j \rightarrow -\infty.$$

Upon substituting Eq. (31b) into Eq. (36) and dropping the argument t, we obtain γ_d as defined by Eq. (14). Let us further postulate the two expressions γ_a and γ_c as defined in Eqs. (11) and (13). Note that from Eq. (13), $\gamma_c[C_d(v_j) + C_j(v_j)] = I_s[\exp\left(\frac{v_j}{V_T}\right) - 1] - i$. Hence, γ_c is equal to $-d\ v_j/dt$ of the two-capacitor model. Also observe that when $v_j > 0$, and $i < 0$. Eq. (11) becomes

$$\gamma_a = \frac{i}{C_j(v_j)} \tag{37}$$

which is the most negative among $\gamma_a, -\gamma_c$, and $-\gamma_d$ since $C_j(v_j)$ is very small (typically in the order of 10^{-11} farad). Hence the function max $(\gamma_a,\ \gamma_b)$ must give γ_b when $v_j > 0$ and $i < 0$, where γ_b is as defined in Eq. (12); namely, $\gamma_b \triangleq - \max(\gamma_c,\ \gamma_d)$. Observe that when $v_j > 0$, the function max$(\gamma_a,\ \gamma_b)$ actually selects between the greater of two possible values of $\left|\frac{dv_j}{dt}\right|$; namely that predicted by γ_c which coincides with the two-capacitor model prediction, or that predicted by Eq. (14) which is based on our postulate of Eq. (32). Consequently, the relationship between the normalized storage time t_s/τ and the reverse-to-forward current ratio I_r/I_f as predicted by the memristive diode model could approach the ideal relationship shown in Fig. 3 by an optimum choice of the model parameter β. On the other hand, when $v_j < 0$ and $i < 0$, Eq. (14) gives-- except when i has decayed to a very small value-- too large a value for dv_j/dt because the exponential term in the denominator approaches

zero when $v_j < 0.$ [14] Moreover, since

$$C_d(v_j) = \frac{I_s \tau}{V_T} \exp\left(\frac{v_j}{V_T}\right) \approx 0$$

and

$$I_s [\exp\left(\frac{v_j}{V_T}\right) - 1] \approx - I_s$$

when $v_j < - V_T < 0$, Eq. (13) can be approximated by

$$\gamma_c \approx \frac{-i}{C_j(v_j)} \qquad (38)$$

But since C_j is very small, Eq. (38) gives too fast a decaying

rate for $v_j(t)$ and $i(t)$. Physically, it is the residual stored charge

in the base-- which can still support a rather large value of $|i(t)|$--

which prevents $i(t)$ from decaying too fast after $t = t_o + t_s$. To

account for this effect, the function $\gamma_a(\cdot)$ as defined in Eq. (11) is

postulated.

---

[14] To see this, we follow a similar procedure used for deriving Eq. (33)
by substituting $\beta = 1$, $i(t_o) = - I_r = - I_f$, and $t = t_s$ into Eq. (14):

$$- \frac{d\ v_j(t_s)}{dt} \approx \frac{V_T\ \bar{p}_n'(0,t_o)}{p_{no} \times 2 \times 0.25\tau} = \frac{V_T\ \bar{p}_n'(0)}{p_{no} \times 0.5\tau}$$

Now $\bar{p}_n'(0)/p_{no} \approx \exp\left[\frac{v_j(t_o)}{V_T}\right]$, and typically $v_j(t_o) \approx 0.7$ volt. Hence

$\bar{p}_n'(0)/p_{no} \approx 5 \times 10^{11}$, and

$$- \frac{d\ v_j(t_s)}{dt} \approx \frac{V_T \times 5 \times 10^{11}}{0.5\ \tau} = \frac{10^{12}\ V_T}{\tau}$$. This is obviously a

much greater decaying rate than that actually observed.

When $v_j < 0$, Eq. (11) reduces to:

$$\gamma_a = \cfrac{i}{C_j(v_j)\left\{1 + \alpha\left[\cfrac{|q_m| + I_s\tau}{(|i| + I_s)\tau}\right]\right\}} \qquad (39)$$

Observe that for sufficiently large value of α, $|\gamma_a|$ will be sufficiently small such that the function $\max(\gamma_a, \gamma_b) = \gamma_a$ when $v_j < 0$ and $i_j < 0$. For a particular diode the value of the empirical parameter α is chosen so that the fall time t_f approximates the measured value as accurately as possible. To demonstrate how sensitive the parameter α is in controlling the fall time, we simulated the circuit shown in Fig. 2(a) with $E_2 = 10$ volts, $R = 1K$, $I_r \approx I_f = 10$ mA, and with α varying from $\alpha = 0.5$ to $\alpha = 10$.[15] The result as summarized in Fig. 8 shows that it is easy to vary α so that a realistic fall time t_f is predicted.

The preceding derivations show our model is indeed capable of mimicking the essential qualitative diode behaviors under both reverse and forward transients. We now turn to some specific examples so that the quantitative behavior can be evaluated.

IV. EVALUATION OF THE MODEL

Consider a silicon diode with the following prarmeters:

$N_D = 10^{15}$ cm^{-3} $\qquad\qquad\qquad$ $\tau_p = 10^{-7}$ sec

$\mu_n = 1350$ cm^2/v-sec. $\qquad\qquad$ $w_n = 5\ L_p$

$\mu_p = 480$ cm^2/v-sec. $\qquad\qquad$ $T = 300^\circ$ K

$I_s = 1/2 \times 10^{-12}$ amp $\qquad\qquad$ $\psi_o = 0.9$ volt

---

[15]Other diode parameters are taken to be the same as those in the examples in Section IV.

From these parameters, we obtain

$$D_p = \mu_p V_T = 12.5 \text{ cm}^2/\text{sec}$$

$$L_p = \sqrt{D_p \tau_p} = 1.12 \times 10^{-3} \text{cm}$$

$$n_{no} \approx N_D = 10^{15} \text{ cm}^{-3}$$

$$P_{no} \approx \frac{n_i^2 (300^\circ K)}{n_{no}} = 2.1 \times 10^5 \text{ cm}^{-3}$$

and[16]

$$A = \frac{I_s L_p}{q D_p P_{no} \coth\left(\frac{W_n}{L_p}\right)} = 1.40 \times 10^{-1} \text{ cm}^{-2}$$

1. Model Testing:

A. Reverse transient:

The above diode is used in the circuit shown in Fig. 2(a). As before we assume the switch S is thrown from right to left at $t = t_o = 0$, and that before $t = 0$, the diode is at steady state with current $i = I_f = 10$ mA. The voltage E_2 is taken to be 10 volts. In all cases α is chosen to be unity, and β is chosen to be 1.5.

The computer simulated result is shown in Figs. 9 and 10. Observe the small voltage drop at $t = 0$ when S is switched. This is because the reverse diode current $-i_r$ as well as $i_2 = \dfrac{q_m(t=0)}{\tau} = \dfrac{I_f \tau}{\tau} = I_f$ both flow

---

[16] It follows from the ideal junction diode law and Eq. (25) that

$$i = I_s[\exp \frac{v_i}{V_T} - 1] = \frac{Aq D_p \coth\left(\frac{W_n}{L_p}\right)}{L_p}, \quad p'_n(0) = \left[\frac{Aq D_p \coth\left(\frac{W_n}{L_p}\right)}{L_p}\right] P_{no}[\exp\left(\frac{v_i}{V_T}\right) - 1]$$

Hence, $I_s = \dfrac{Aq D_p \coth\left(\frac{W_n}{L_p}\right) P_{no}}{L_p}$, or $A = \dfrac{I_s L_p}{q D_p P_{no} \coth\left(\frac{W_n}{L_p}\right)}$

through the memristor from minus to plus terminal (see Fig. 5(b)) and cause

the small instantaneous drop in the voltage waveform. Also observe that

the voltage waveform v(t) before $t = t_s$ is almost flat (so is

$i(t) \simeq - [E_2 + v(t)]/R$). This will be obvious if we look at the case

$I_r = I_f$ as described by Eq. (33) where we have[17]

$$\frac{dp_n'(0)}{dt} = - K, \text{ K being a positive constant.}$$

This means that $p_n'(0)$ decreases linearly with time t before $t = t_s$.

But

$$v_j = V_T \ln [1 + \frac{p_n'(0)}{P_{no}}] \tag{40}$$

It follows from Eq. (40) that as $p_n'(0)$ decreases linearly with t, $v_j(t)$

will decrease very slowly. For $t > t_s$, $v_j(t) < 0$, and $\frac{dv_j}{dt} = \gamma_a$. Hence,

$\frac{dv_j}{dt}$ must decay in accordance with Eq. (39). The current i(t) must also

decay correspondingly, and as i(t) approaches zero, the voltage drop

across the memristor becomes negligible.

In Fig. 3 we show the normalized storage time t_s/τ predicted by

different models as a function of the reverse-to-forward current ratio

I_r/I_f. We see that the memristive model gives an excellent approximation.

B. Forward transient:

The above same diode is now used in the circuit shown in Fig. 4(a).

Different current steps are applied and the computed voltage transient

---

[17]Although we assumed $\beta = 1$ in the derivation of Eq. (33), it does not
matter here since we are only trying to develop some intuitive feeling
for the model.

waveforms are shown in Fig. 11. Observe that the waveforms behave exactly as described in Section I-B. The reason for the success of this model can be explained _intuitively_ as follows.

Recall that when $i > 0$, $I_1 = I_{1f}$; i.e.,

$$I_1 = I_s \ [\exp\left(\frac{v_j}{v_T}\right) - 1] + C_d(v_j) \ \frac{dv_j}{dt} \ .$$

Thus our model reduces to that shown in Fig. 12. Now when I_f is small, capacitors C_j and C_d will charge slowly, and $v_m = I_f \ R_m(q_m)$ is negligible. Hence we expect to obtain the lowermost waveform in Fig. 11. When I_f is large, capacitors C_d and C_j will charge rapidly and $v_j(t)$ will also rise rapidly. Moreover, at the instant when this large I_f is applied,

$q_m(t=0) = 0$, $i_2(t=0) = \frac{q_m}{\tau} = 0$, and all I_f must consequently flow through the memristor $R_m(q_m)$ whose resistance is relatively very high. Hence, an initial jump of $v_m = R_m(0) \ I_f$ volts occurs at $t = 0$. As time increases, however, the memristor charge, $q_m(t)$, increases and its resistance $R_m(q_m)$ decreases accordingly (See Fig. 6). Simultaneously, the memristor voltage $v_m(t) = i_m(t) \ R_m(q_m(t))$ decreases while the current $i_2 \ (q_m)$ increases (this further reduces $i_m(t)$, hence $v_m(t)$) until $i_2(q_m) = I_f$, when $v_m(t) = 0$ (since $i_m(t) = I_f - i_2(q_m) = 0$). Thus with $v_j(t)$ rising rapidly to its steady state value while $v_m(t)$ decreases quickly to zero, we obtain the uppermost waveform in Fig. 11. The two components $v_j(t)$ and $v_m(t)$ and their superposition, $v(t) = v_j(t) + v_m(t)$, are depicted qualitatively in Fig. 13 (a), (b), and (c) for large, intermediate, and small magnitudes of the current step I_f, respectively.

From the above two examples we see that the memristor $R_m(q_m)$
is responsible for the conductivity modulation phenomenon--which is
so important during forward transient-- as well as for the initial
small voltage drop during reverse transient.

C. Sinusoidal response in rectifying circuits:

The circuits shown in Figs. 14(a) and 15(a) have been simulated
in the computer. The results are shown in Figs. 14(b) and 15(b),
respectively. We observe that in each case there is a small 'tail'
in the current waveform in the cut-off half cycle. This is obviously
due to the effect of the charge stored in the base. In fact, our
computed results agree remarkably well with the real observations given
in [14].

2. Small Signal Impedance:

Assume that a junction diode is under forward bias. Under this
condition ($i > 0$) we have already shown that our memristive diode model
is equivalent to the circuit shown in Fig. 12. Since $C_d \gg C_j$ under
forward bias, we can neglect C_j for simplicity. Let us apply a steady
current source I_{in} upon which a small signal $i_{in}(t)$ is superimposed as
shown in Fig. 16. Throughout this section, we use upper case letter
(I, V_m, etc.) to denote the dc component of a variable, lower case letter
to denote the ac component, and capital script letter to denote the
total instantaneous value. We put a wiggle "~" on top of a variable to denote
its Laplace transformation. Using the above notations, the impedance $\tilde{Z}_1$
of the upper part of the memristive diode circuit model shown in Fig. 16
is given by:

$$\tilde{Z}_1 = \frac{1}{\frac{1}{r_j} + j\omega C_d} = \frac{r_j}{1 + j\omega r_j C_d} \qquad (41)$$

The incremental resistance r_j and capacitance C_d about the dc operating point $\tilde{V}_j = V_j$ are given by:

$$r_j \triangleq \left(\frac{dI_j}{dv_j}\right)^{-1} = \left[\frac{d}{dV_j}\left\{I_s\left[\exp\left(\frac{V_j}{V_T}\right) - 1\right]\right\}\right]^{-1}$$

$$= \left[\frac{I_s}{V_T} \exp\left(\frac{V_j}{V_T}\right)\right]^{-1} = \left[\frac{I_s + I_j}{V_T}\right]^{-1} \qquad (42)$$

and

$$C_d = \frac{I_s \tau}{V_T} \exp\left(\frac{V_j}{V_T}\right) = \frac{\tau(I_s + I_j)}{V_T} \qquad (43)$$

substituting Eqs. (42) and (43) into Eq. (41) we obtain:

$$\tilde{Z}_1 = \frac{V_T (1 - j\omega\tau)}{(I_s + I_j)(1 + \omega^2\tau^2)} \qquad (44)$$

The impedance $\tilde{Z}_2$ of the lower part of the memristive diode circuit model is derived as follows: At steady state $I_{in} = I_j = I_2 = I$ (where we have denoted the steady current as I) and $I_m = 0$. Moreover, observe that

$$\vartheta_2 = \frac{Q_m}{\tau} = \frac{\int_0^t \vartheta_m(t')dt'}{\tau}$$

Hence $\quad i_m = \vartheta_m = \tau \frac{d\vartheta_2}{dt} = \tau \frac{di_2}{dt} \qquad (45)$

It follows that $\vartheta_{in} = I + i_{in} = \vartheta_2 + \vartheta_m = I + i_2 + \tau \dfrac{di_2}{dt}$

and $i_{in} = i_2 + \tau \dfrac{di_2}{dt}$. Therefore, $\tilde{i}_{in} = \tilde{i}_2 + \tau s\, \tilde{i}_2$, or

$$\frac{\tilde{i}_2}{\tilde{i}_{in}} = \frac{1}{1 + \tau s} = \frac{1}{1 + j\omega\tau} \tag{46}$$

Now

$$\tilde{v}_m = \tilde{i}_m R_m = \left[\tau \frac{\widetilde{di_2}}{dt}\right] R_m = \tau s\, \tilde{i}_2 R_m = j\omega\tau\, \tilde{i}_2 R_m$$

Hence

$$\tilde{Z}_2 \triangleq \frac{\tilde{v}_m}{\tilde{i}_{in}} = j\omega\tau R_m \frac{\tilde{i}_2}{\tilde{i}_{in}} = \frac{j\omega\tau R_m}{1 + j\omega\tau} = \frac{R_m(j\omega\tau + \omega^2\tau^2)}{1 + \omega^2\tau^2} \tag{47}$$

Adding Eqs. (44) and (47) we obtain the total impedance

$$\boxed{\tilde{Z} = \tilde{Z}_1 + \tilde{Z}_2 = \frac{V_T + (I+I_s)\,\omega^2\tau^2 R_m}{(I_s+I)(1 + \omega^2\tau^2)} + \frac{j\omega\left[\tau R_m - \dfrac{\tau\,V_T}{I_s + I}\right]}{1 + \omega^2\tau^2}} \tag{48}$$

It follows from Eq. (48) that if I is small such that $R_m \ll \dfrac{V_T}{I_s + I}$, then the reactive component of $\tilde{Z}$ is negative and the impedance is predominantly <u>capacitive</u>. Similarly if I is large such that $R_m \gg \dfrac{V_T}{I_s + I}$, then the impedance is predominantly <u>inductive</u>. These properties are consistent with those alluded to in Section I-B.

3. The Memristive Diode Model at Steady State:

It is also interesting to observe that under steady state condition, we have $i_j = i_m = 0$ (see Fig. 5(b)). Hence, using the same notation as

in the preceding section, we have:

$$I_1 = I_2 = I \tag{49}$$

where I denotes the steady state diode current. It follows from $I_2 = \dfrac{Q_m}{\tau}$ and Eq. (23) that

$$\frac{Q_m}{\tau} = \frac{Q'_p}{\tau} = \left[\frac{Aq\ D_p\ P'_n(0)}{L_p}\ \coth\left(\frac{W_n}{L_p}\right)\right]\left\{\frac{[1 - \text{sech}\left(\frac{W_n}{L_p}\right)]\ \tau_p}{\tau}\right\}$$

$$= \frac{Aq\ D_p\ P'_n(0)}{L_p}\ \coth\left(\frac{W_n}{L_p}\right) = I_s[\exp\left(\frac{V_j}{V_T}\right) - 1] \tag{50}$$

where we have made use of Eq. (6) and the relations:

$$I_s = \frac{Aq\ D_p\ \coth\left(\frac{W_n}{L_p}\right)}{L_p}\ P_{no}$$

and

$$P'_n(0) = P_{no}[\exp\left(\frac{V_j}{V_T}\right) - 1]$$

Finally, it follows from Eqs. (49) and (50) that:

$$I = I_1 = I_2 = I_s[\exp\left(\frac{V_j}{V_T}\right) - 1] \tag{51}$$

Thus the memristive diode model reduces to just a nonlinear resistor obeying the diode junction law, as any valid diode model should.

V. CONCLUDING REMARKS

A new p-n junction diode model containing only 4 lumped circuit elements has been presented. Each component of this model bears a simple relationship with the physical operating mechanisms inside the diode. In spite of its simplicity, this model is shown capable of simulating realistically the diode's dynamic behaviors under reverse, forward, and sinusoidal operating modes.

During reverse transient operation, the model yields a normalized storage time t_s/τ vs. I_r/I_f relationship which is far more accurate than that predicted by the standard two-capacitor model (and Barna-Horelick model), or the Linvill two-lumped model (and Wang-Branin two-lumped model). This model is also shown capable of mimicking realistically the reverse transient decay behaviors. By adjusting a single emperical parameter, the fall time t_f can be predicted accurately. To obtain a comparable accuracy using the Linvill or the Wang-Branin model would have required typically 20 multi-lumped sections [4].

During forward transient operation, the model is shown capable of simulating all known qualitative behaviors. In particular, the model's voltage response to a current step input $i = I_f\, U(t)$ is shown to be monotonically increasing when I_f is small and monotonically decreasing, after an initial overshoot, when I_f is large. For intermediate values of I_f, a highly damped oscillatory response is observed.

The model is also shown to correctly predict the diode's small-signal behaviors; namely, the model exhibits a predominantly capacitive impedance when the biasing current I_f is small, and a predominantly inductive impedance when I_f is large. Finally, the model reduces in the

steady state to a single nonlinear resistor characterized by the ideal junction law.

The success of this new model is due largely to the use of the memristor which accounts for the charge-storage and conductivity modulation effects. It appears that memristors are useful for modeling other devices which exhibit delay and charge storage effects. In particular, the techniques presented in this paper should be applicable also to the modeling of the p-i-n diode [15] or the step-recovery diode [16]. Memristors have also been used successfully to model mechanical and electro-chemical devices [17].

In view of its rather recent origin, a theoretical analysis of circuits containing memristors might appear to be a difficult task [18]. However, from the computer-aided circuit analysis point of view,[18] the memristive diode circuit model is quite attractive because it is simple, realistic, and requires very little computer memory.

---

[18] The expressions defining the controlled source i_1 may appear to be rather complicated. However, since these expressions do not involve any time differentiation, their numerical evaluation require no more than simple algebraic computations, a task well suited for a computer.

APPENDIX

A. Governing Equations for Two-Capacitor Model in Reverse Transient:

For $t \leq t_o + t_s$, $v_j(t) \geq 0$ and $i(t) \doteq -I_r$. If we neglect C_j in the two-capacitor model,[19] the resulting model is shown in Fig. A1, where we see that

$$-I_r = i = I_s \left[\exp\left(\frac{v_j}{V_T}\right) - 1 \right] + C_d(v_j) \frac{dv_j}{dt}$$

$$= \frac{\tau I_s \left[\exp\left(\frac{v_j}{V_T}\right) - 1 \right]}{\tau} + \frac{\tau I_s}{V_T} \exp\left(\frac{v_j}{V_T}\right) \frac{dv_j}{dt} \qquad (A.1)$$

It follows from footnote 16 and Eq. (23) that

$$I_s = \frac{Aq \, D_p \coth\left(\frac{W_n}{L_p}\right) P_{no}}{L_p} \qquad (A.2)$$

and

$$q_p' = \frac{Aq \, D_p \coth\left(\frac{W_n}{L_p}\right)}{L_p} P_n'(0) \, \tau$$

$$= \tau \frac{Aq \, D_p \coth\left(\frac{W_n}{L_p}\right) P_{no}}{L_p} \left[\exp\left(\frac{v_j}{V_T}\right) - 1 \right]$$

$$= \tau \, I_s \left[\exp\left(\frac{v_j}{V_T}\right) - 1 \right] \qquad (A.3)$$

---

[19] This assumption is valid since $C_d(v_j) \gg C_j(v_j)$ when $v_j > 0$.

substituting Eq. [A.3] into Eq. (A.1), we obtain

$$-I_r = \frac{q_p'}{\tau} + \frac{dq_p'}{dt}$$ (A.4)

which is the equation alluded to in footnote 3 for a <u>long base</u> diode ($\tau = \tau_p$).

B. <u>Smooth Approximation of U(x)</u>:

Define

$$\hat{U}(x, K, \delta) \triangleq \frac{1}{1 + (K)^{\frac{-x}{|x|+\delta}}}$$ (B.1)

where K and δ are positive constants to be chosen for the desired accuracy (K should be large while δ should be small). The curve representing the function $\hat{U}(\cdot, K, \delta)$ is shown qualitatively in Fig. B.1 as a function of δ. Observe that as $\delta \to 0$, and $K \to \infty$, $\hat{U}$ tends to the <u>unit step function</u>.

It is easy to show that $\hat{U}(x, K, \delta)$ is differentiable with respect to x.

C. <u>Smooth Approximation of max (x,y)</u>.

Define

$$g(x, K, \delta) \triangleq x \, \hat{U}(x, K, \delta)$$ (C.1)

where K and δ are defined above. Observe that

$$g(x, K, \delta) \approx x, \qquad x > 0$$
$$\approx 0, \qquad x < 0$$ (C.2)

Hence, $g(\cdot, K, \delta)$ represents an excellent approximation to a <u>unit ramp function</u> as shown in Fig. C1. If we define

$$\hat{M}(x, y, K, \delta) \triangleq x + g(y-x, K, \delta) \tag{C.3}$$

then

$$\hat{M}(x, y, K, \delta) \approx \begin{cases} x & \text{if } x > y \\ y & \text{if } x < y. \end{cases} \tag{C.4}$$

A curve representing $\hat{M}(x_a, y, K, \delta)$ is shown in Fig. C2.

REFERENCES

1. N. O. Sokal, J. J. Sierakowski, and J. J. Sirota, "Modeling transistors and diodes for computer-aided nonlinear circuit analysis," _Electronic Design_, Part 1, June 7, 1967, pp. 54-59; Part 2, June 21, 1967, pp. 60-66; and Part 3, July 5, 1967, pp. 80-83.

2. A. A. Barna and D. Horelick, "A simple diode model including conductivity modulation," _IEEE Trans. on Circuit Theory_, vol. CT-18, pp. 233-240, March 1971.

3. J. G. Linvill, _Models of Transistors and Diodes_, New York: McGraw-Hill, 1963.

4. P. P. Wang and F. H. Branin, Jr., "Multi-section network modeling of junction diodes," Proceeding of the 4th Annual Pittsburg Conference on Modeling and Simulation, Pittsburg, Penn., May 1973.

5. L. O. Chua, "Memristor--the missing circuit element," _IEEE Trans. on Circuit Theory_, vol. CT-18, pp. 507-519, September 1971.

6. P. E. Gray, D. DeWitt, A. R. Boothroyd, and J. F. Gibbons, _Physical Electronics and Circuit Models of Transistors_, New York: Wiley, 1964.

7. W. H. Ko, "The forward transient behavior of semiconductor junction diodes," _Solid State Electronics_, vol. 3, pp. 59-69, 1961.

8. H. L. Armstrong, "On switching transient in the forward conduction of semiconductor diodes," _IRE Trans. on Electron Devices_, vol. ED-4 pp. 111-113, April 1957.

9. T. E. Firle and O. E. Hayes, "Some reactive effects in forward biased junctions," *IRE Trans. on Electron Devices*, vol. ED-6, pp. 330-334, July 1959.

10. I. Ladany, "An analysis of inertia inductance in a junction diode," *IRE Trans. on Electron Devices*, vol. ED-7, pp. 303-310, October 1960.

11. D. A. Calahan, *Computer-Aided Network Design*, New York: McGraw-Hill, 1972.

12. W. H. Ko, "The reverse transient behavior of semiconductor junction diodes," *IRE Trans. on Electron Devices*, vol. ED-8, pp. 123-131, March 1961.

13. B. Lax and S. F. Neustadter, "Transient response of a p-n junction," *Journal of Applied Physics*, vol. 25, no. 9, pp. 1148-1154, September 1954.

14. J. G. Linvill, "Transient response of junction diodes," *IEEE Trans. on Circuit Theory*, vol. CT-10, pp. 191-197, June 1963.

15. H. M. Olson, "p-i-n Diodes," Chapter 9 of *Microwave Semiconductor Devices and Their Circuit Applications*, Edited by H. A. Watson, New York: McGraw-Hill Book Co., 1969.

16. J. L. Moll, S. Krakauer, and R. Shen, "P-n junction charge-storage diodes," *Proc. of the IRE*, vol. 50, pp. 43-52, January 1962.

17. G. F. Oster and D. M. Auslander, "The memristor: a new bond graph elements," *Journal of Dynamic Systems, Measurements, and Control, Trans. of the ASME*, pp. 249-252, September 1972.

18. Y-F. Lam, "Formulation of normal form equations of nonlinear networks containing memristors and coupled elements," *IEEE Trans. on Circuit Theory*, vol. CT-19, pp. 585-594, November 1972.

Fig. 1.   Existing models of junction diodes: (a) two-capacitor model,

   (b) Barna-Horelick model, (c) Linvill's multi-lumped model, and (d)

   Wang-Branin model.

Fig. 2.   Reverse transient behavior of junction diodes:(a) simplified

   circuit for measuring diode reverse transient (b) the qualitative

   waveforms of diode voltage and current during reverse transient.

Fig. 3.   The relationships between the normalized storage time t_s/τ and

   the reverse-to-forward current ratio I_r/I_f as predicted by different

   models for long base junction diodes.

Fig. 4.   Forward transient behaviors of junction diodes:(a) the simplified

   circuit for measuring diode forward transient, (b) the input current

   step $i_s(t)$ and the qualitative voltage waveforms during forward

   transient corresponding to three different values of I_f.

Fig. 5.   (a) A one-dimensional junction diode (b) the memristive model

   for the diode shown in (a).

Fig. 6.   A typical relationship for the memristor resistance $R_m(q_m)$ as a

   function of the charge q_m passing through its terminals.

Fig. 7.   The qualitative distribution of the carrier concentration $p_n(x)$

   in the base region during reverse transient operations.

Fig. 8.   The current transient waveforms of the circuit in Fig. 2(a)

   with R = 1 KΩ, E_2 = 10 volt, I_f = 10 M.A. and with α varying from

   0.5 to 10.

Fig. 9.   The reverse transient response of a junction diode in the circuit

   shown in Fig. 2(a):   (a) the voltage waveforms corresponding to

different values of R: 0.2K, 0.25K, 0.333K, and 0.5K, (b) the

corresponding current waveforms.

Fig. 10.   Same as Fig. 9 except R = 0.625K, 0.833K, 1.25K, and 2.5K.

Fig. 11.   The forward transient response of the diode in Fig. 4(a).

Fig. 12.   The equivalent circuit of the memristive diode model which

applies when the diode current $i > 0$.

Fig. 13.   The qualitative forward transient waveforms of the voltages

$v(t)$, $v_j(t)$ and $v_m(t)$ across the memristive diode model, the

junction capacitor C_j, and the memristor R_m, respectively:

(a) high input current case (b) intermediate input current case,

and (c) low input current case.

Fig. 14.   The sinusoidal response of a junction diode: (a) the circuit

arrangement, (b) the sinusoidal voltage excitation $e(t) - E_D$, and

the calculated current response $i(t)$.   (The voltage scale is 2

volts per division and the current scale 2 mA per division.)

Fig. 15.   (a) the bridge rectifier circuit, (b) the current waveforms

$i_1(t)$ for D_1 and $i_2(t)$ for D_2 due to the sinusoidal excitation

$e(t)$.   (The voltage scale is 2 volts per division and the current

scale is 2 mA. per division.)

Fig. 16.   Simplified circuit of the memristive diode model driven

by a small ac signal $i_{in}(t)$ superimposed on top of a dc forward

bias I_{in}.

Fig. A1.   Simplified circuit for the two-capacitor model when $v_j > 0$.

Fig. B1.   The smooth function $\hat{U}(x, K, \delta)$ for approximating a step

function is shown qualitatively as a function of x with δ as a

parameter and K fixed.

Fig. C1. The smooth function $g(x, K, \delta)$ for approximating the unit ramp

is shown as a function of x for a typical set of values of δ and K.

Fig. C2. A representative curve $\hat{M}(x_a, \cdot, K, \delta)$ associated with the

smooth function $\hat{M}(x, y, K, \delta)$ for approximating the function

$$\max(x,y) = \begin{cases} x, & x > y \\ y, & x < y \end{cases} .$$
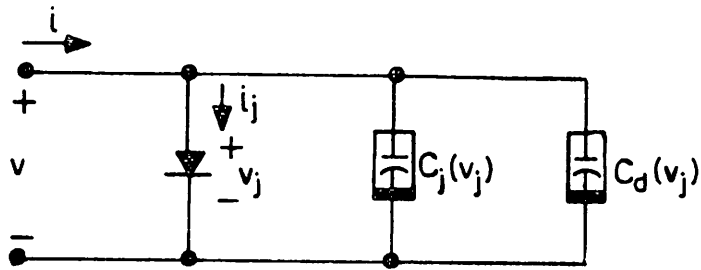
$$i_j = I_s\left[\exp\left(\frac{v_j}{V_T}\right)-1\right] \quad, \quad V_T \triangleq \frac{kT}{q}$$

$$C_j(v_j) = \frac{K_a}{2}\left(\psi_o - v_j\right)^{-1/2}, \quad \psi_o = \text{built-in voltage}$$

$$C_d(v_j) = \frac{I_s \tau}{V_T}\exp\left(\frac{v_j}{V_T}\right), \quad I_s = \text{saturation current}$$

K_a and τ are diode parameters

(a) Two-Capacitor Model
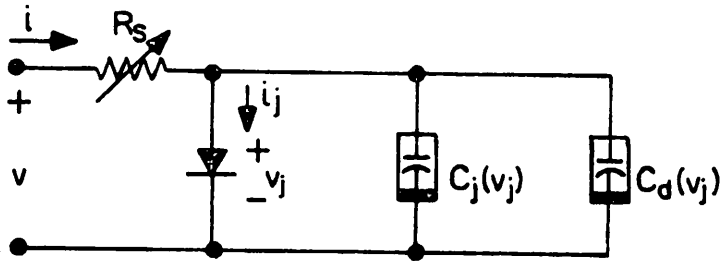
$$R_s = R_o\, f(i_j) \qquad \text{where:}$$

$$f(i_j) \triangleq 1 - \frac{1}{X_n}\ln\frac{1 + K_r i_j}{1 + K_r i_j\, e^{-X_n}}$$

R_o, X_n and K_r are diode parameters

(b) Barna-Horelick Model

(c) Linvill's Multi-Lumped Model

$$P(v) \triangleq P_{n_o}(e^{v_j/V_T}-1)$$

(d) Wang-Branin Model

Fig. I

Fig. 2

Fig. 3

(a)

$I_1 < I_2 < I_3$
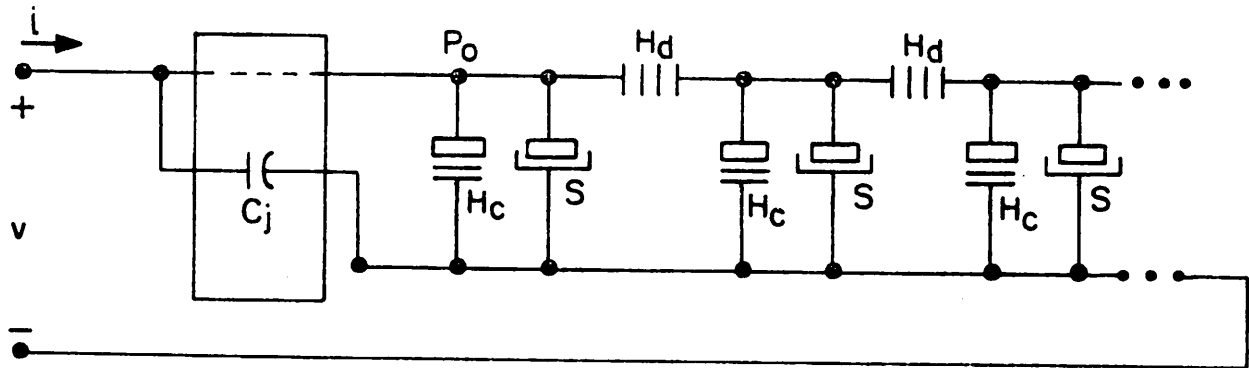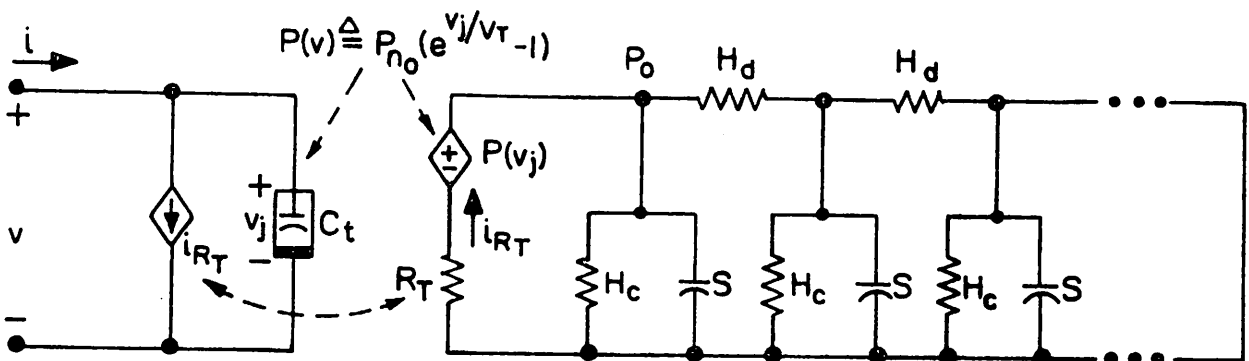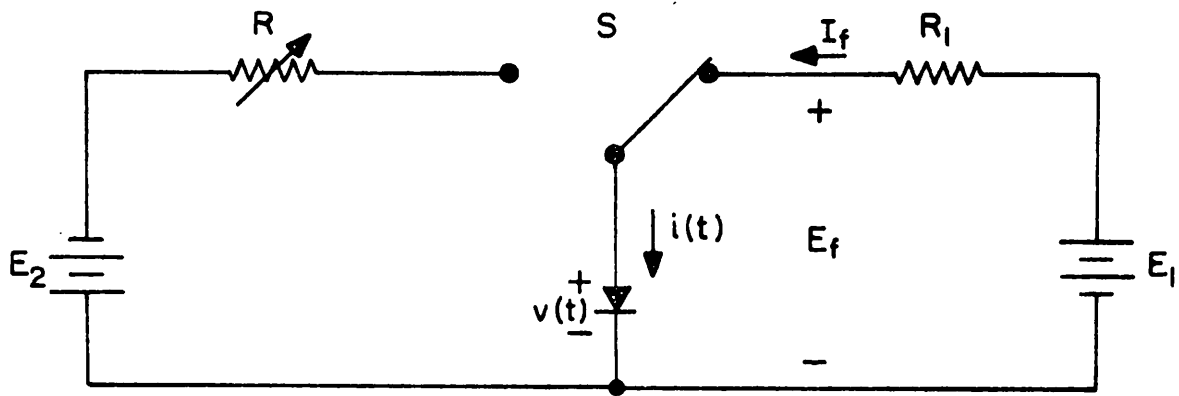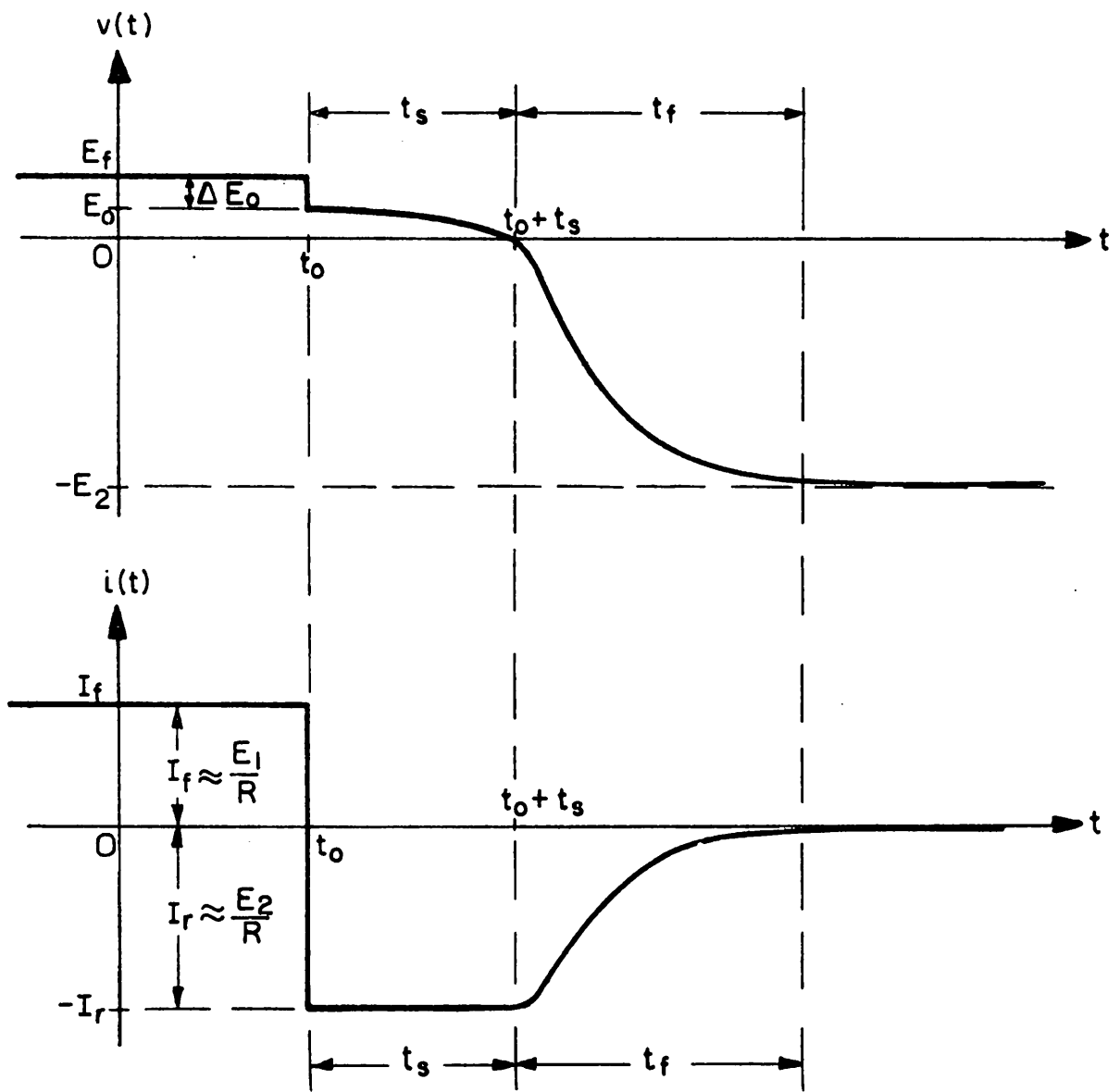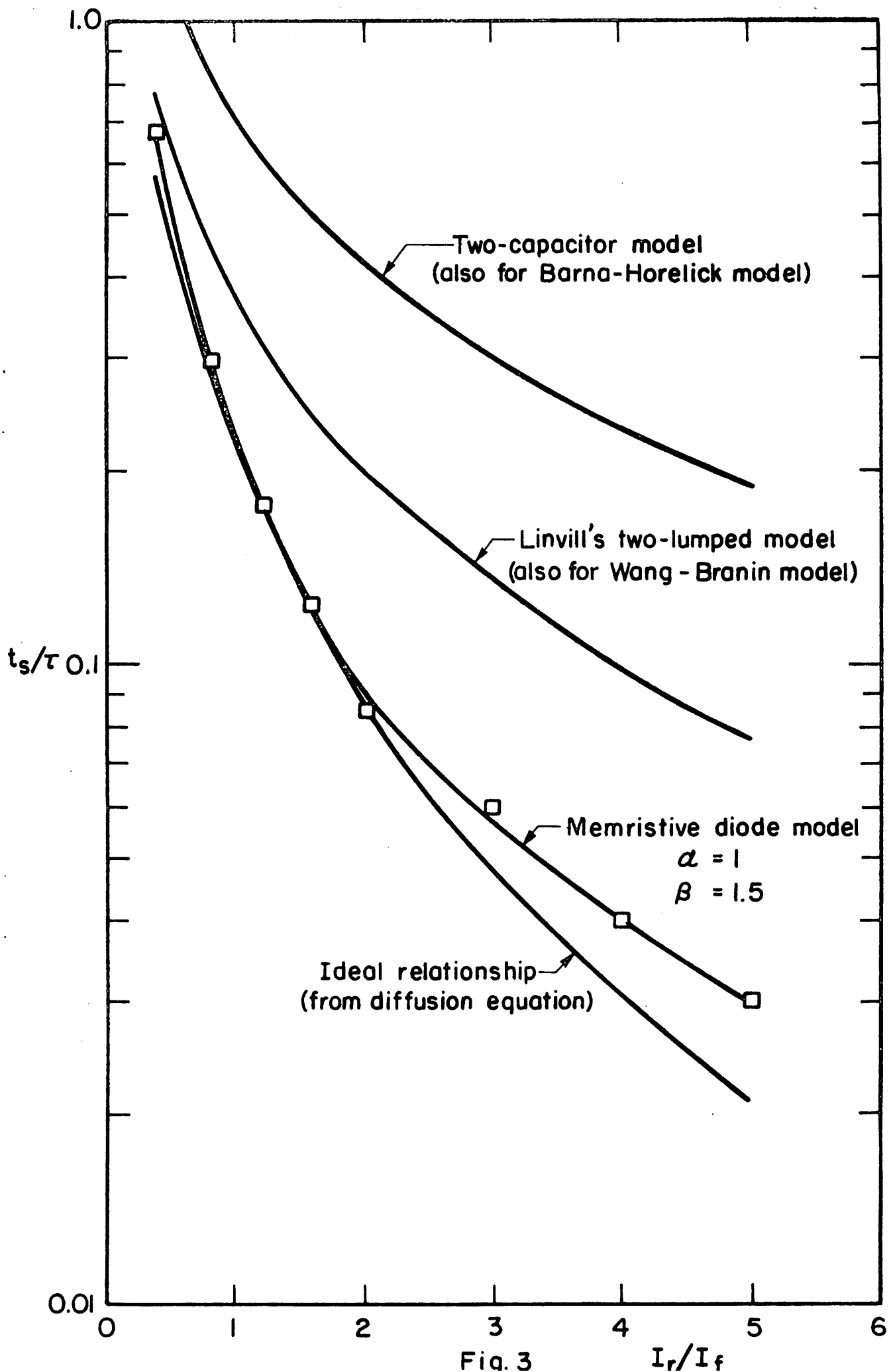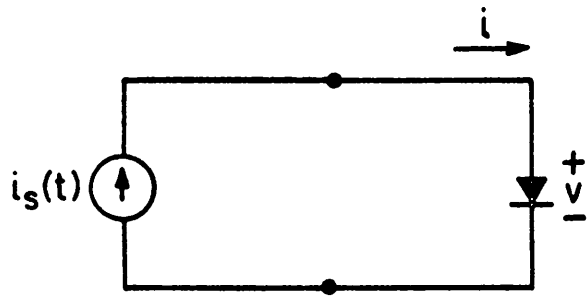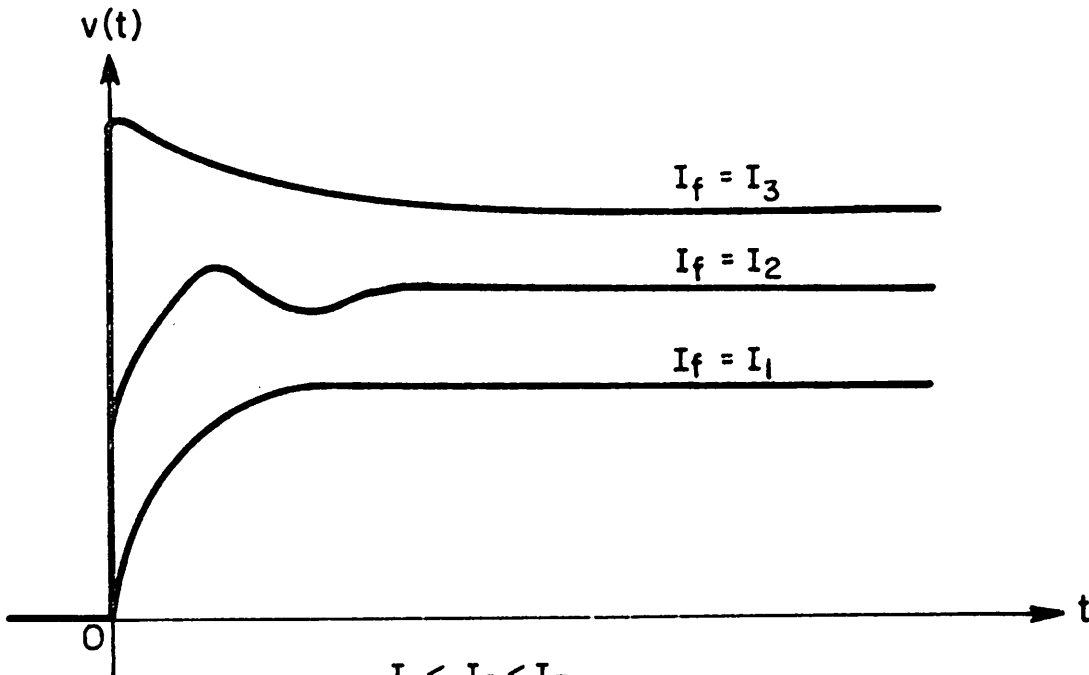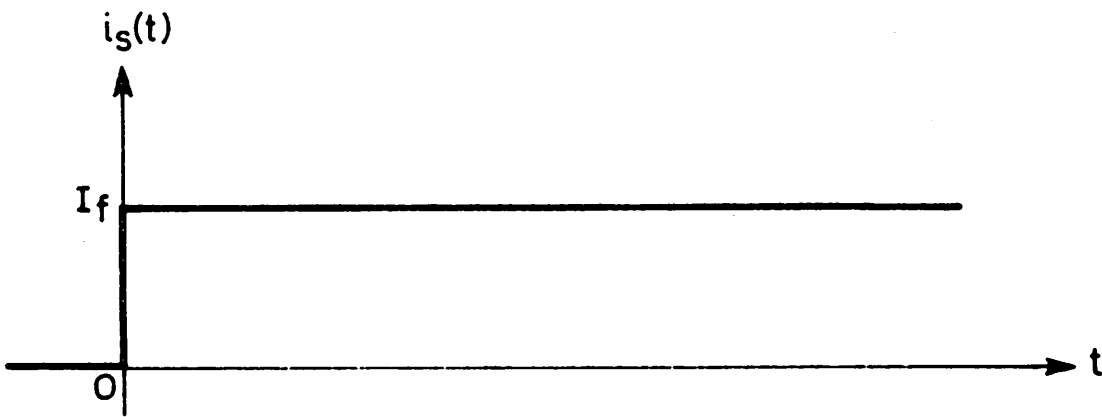
(b)

Fig. 4
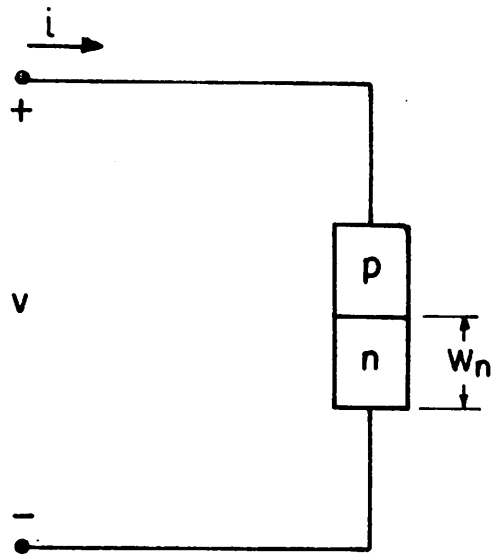
(a)
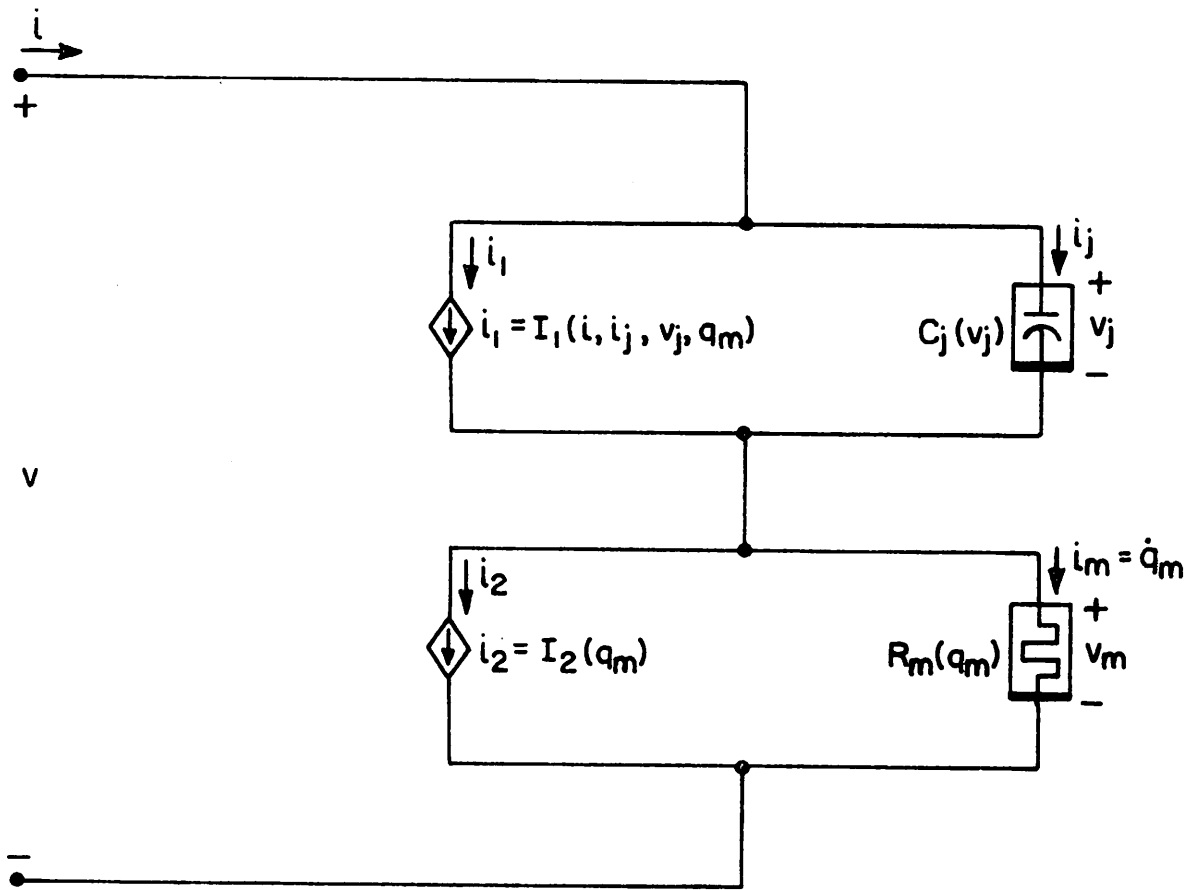
(b)

Fig. 5
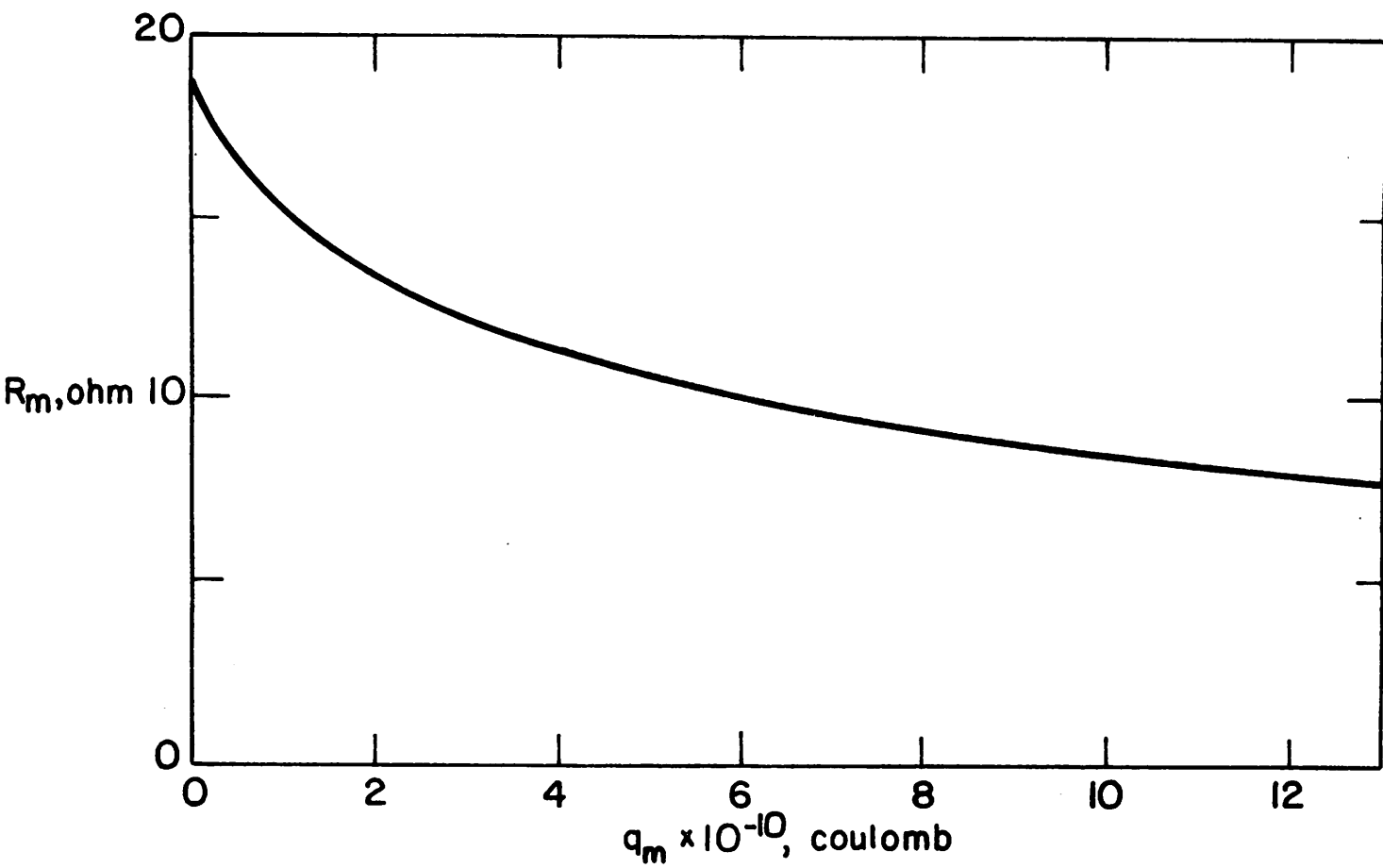
Fig. 6

Fig. 7

Fig. 8

(a)

(b)

Fig. 9

Fig. 10

Fig. 11
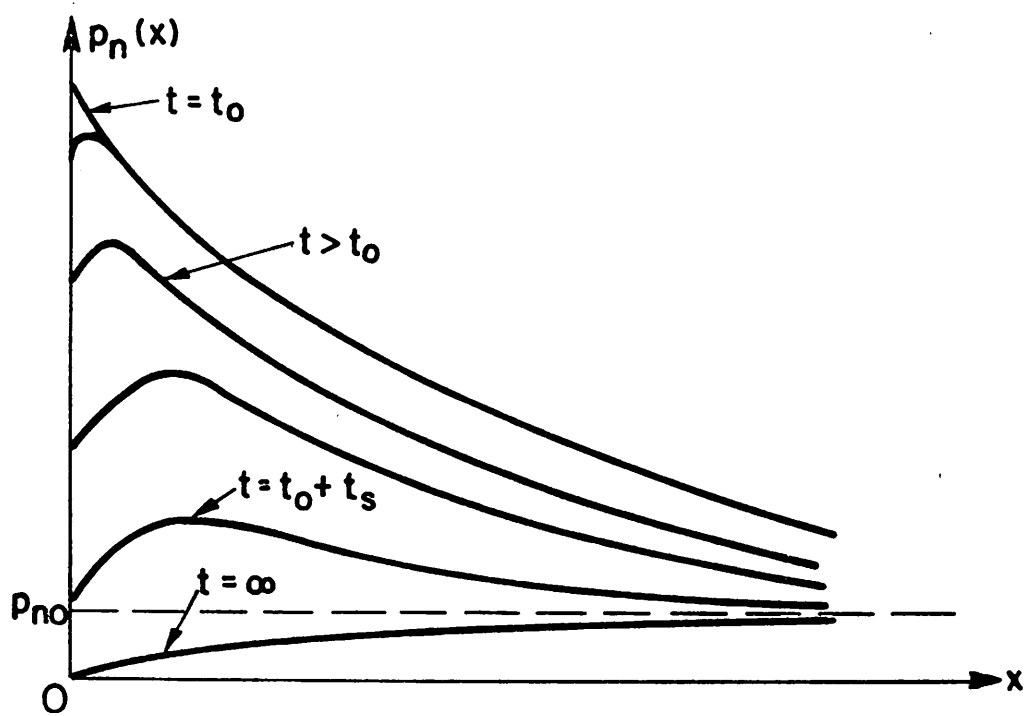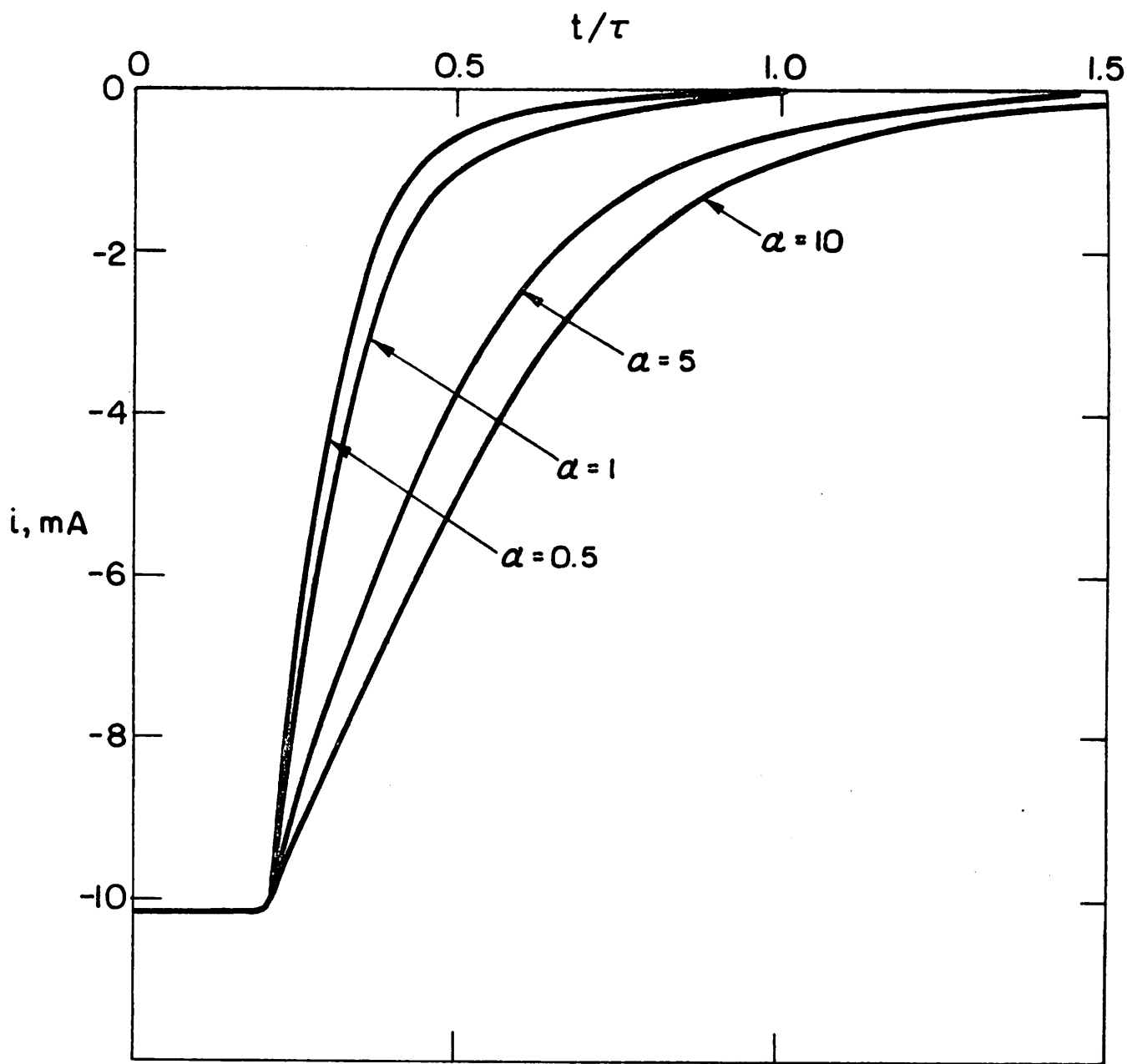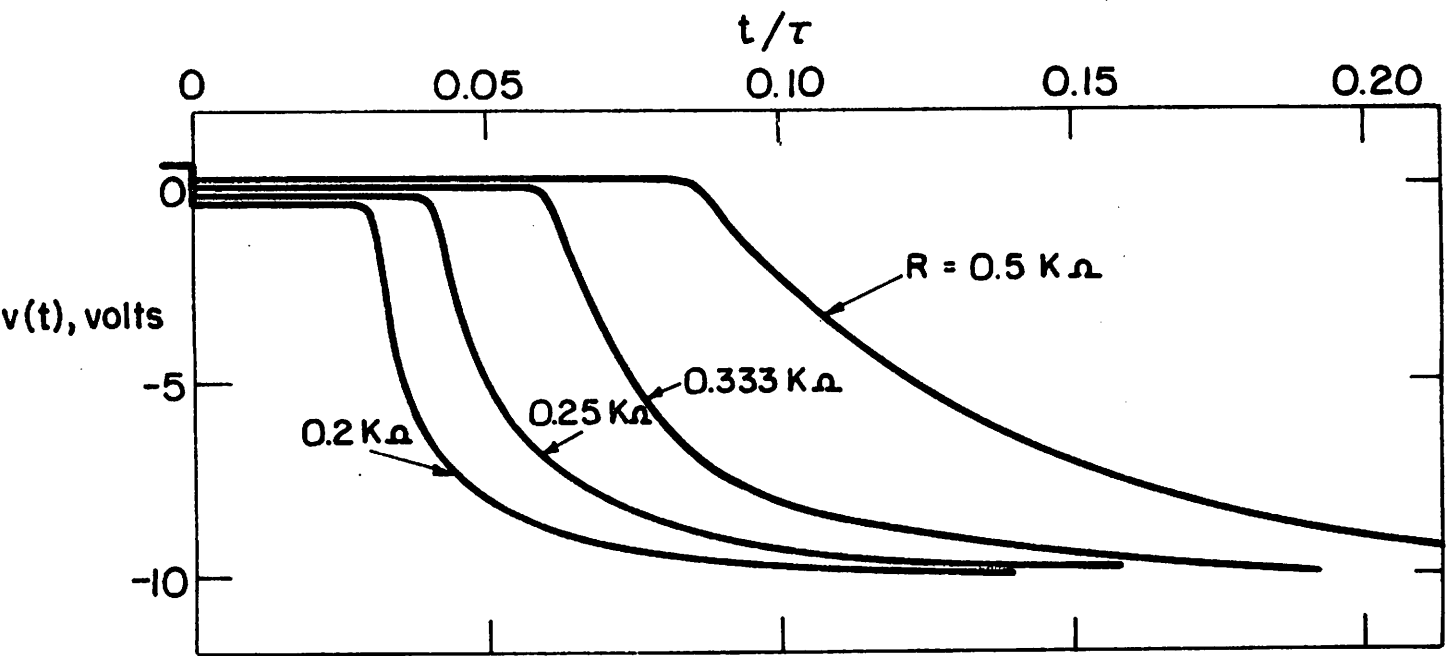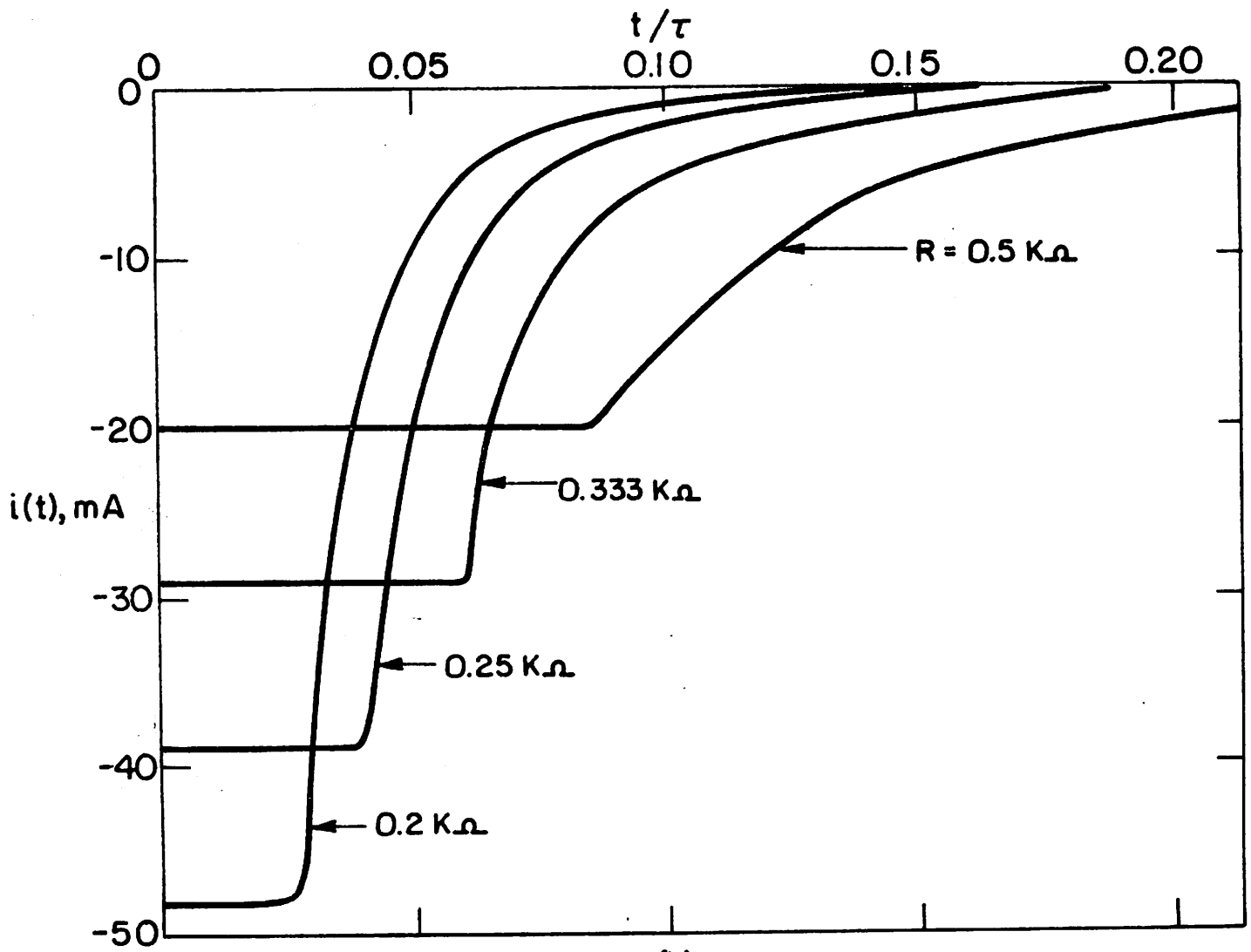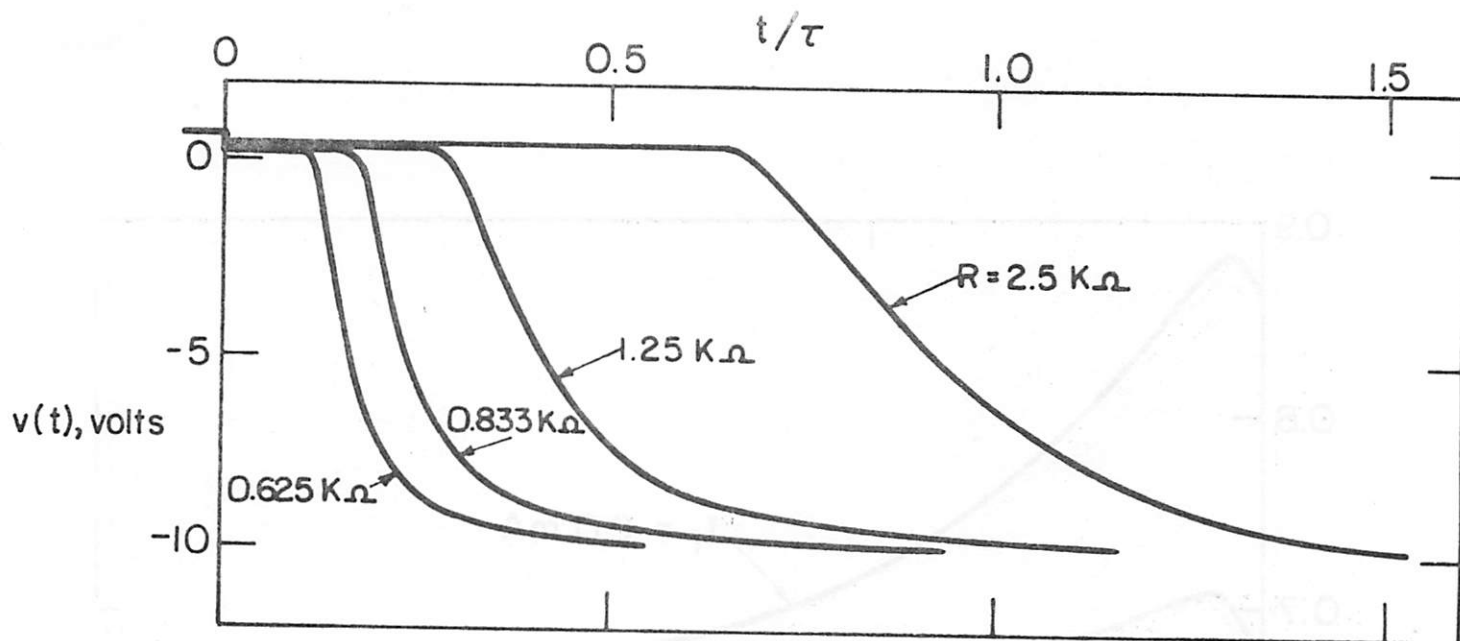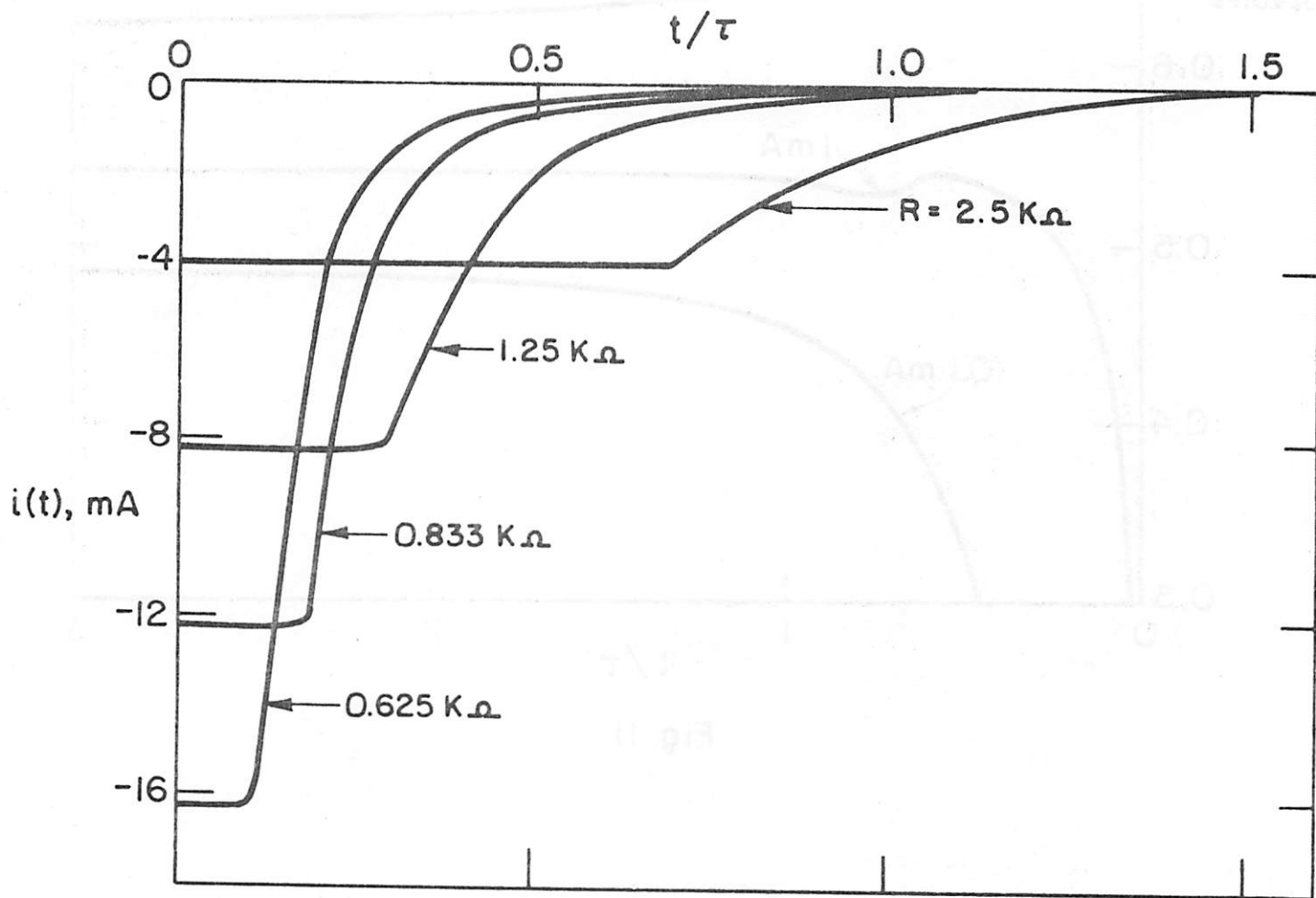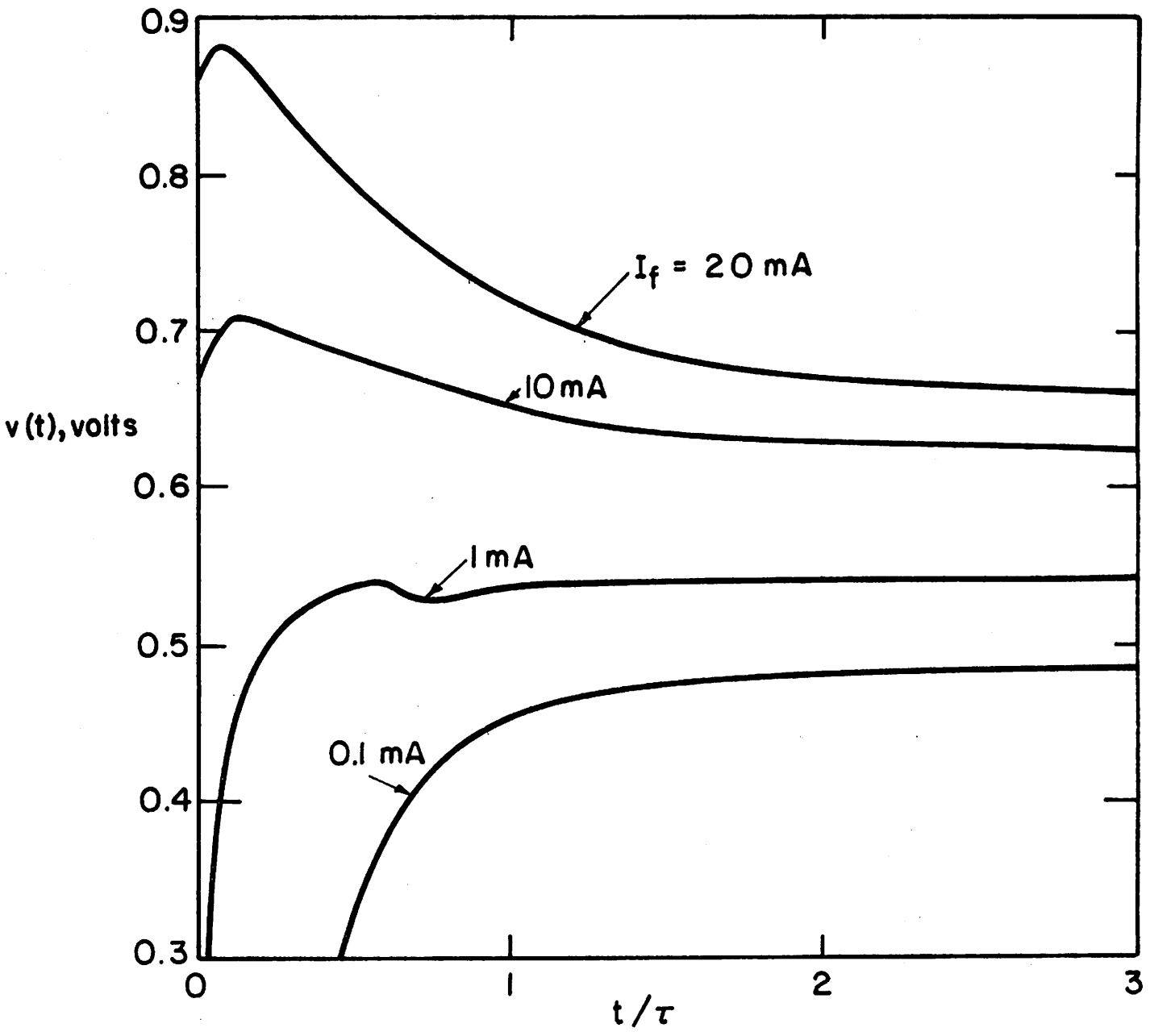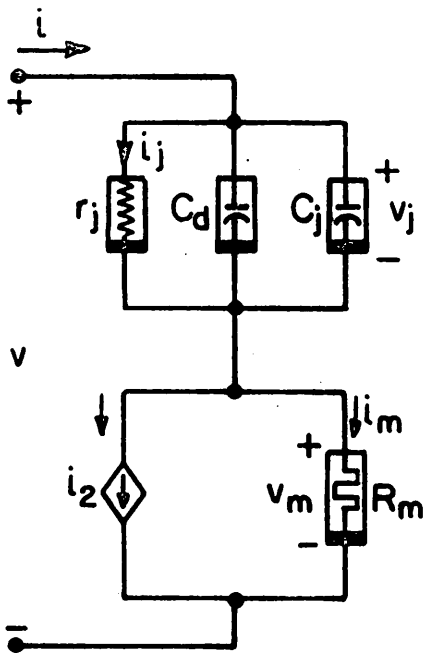
$$r_j = \left(\frac{di_j}{dv_j}\right)^{-1} = \frac{d}{dv_j}\left[I_S\left\{\exp\left(\frac{v_j}{V_T}\right) - 1\right\}\right]^{-1}$$

$$C_d = \frac{\tau I_S}{V_T}\exp\left(\frac{v_j}{V_T}\right)$$

$$i_2(q_m) = \frac{q_m}{\tau}$$

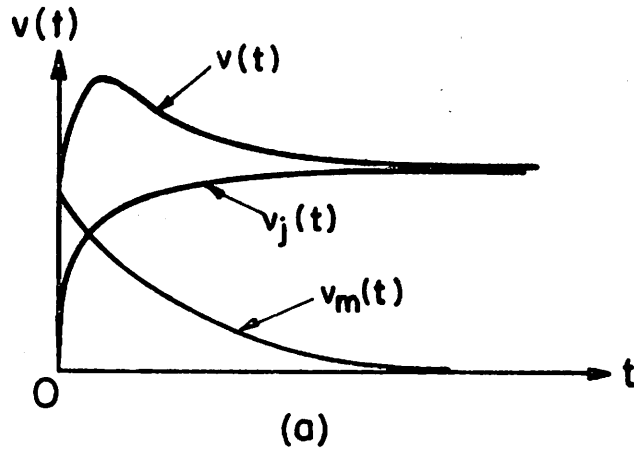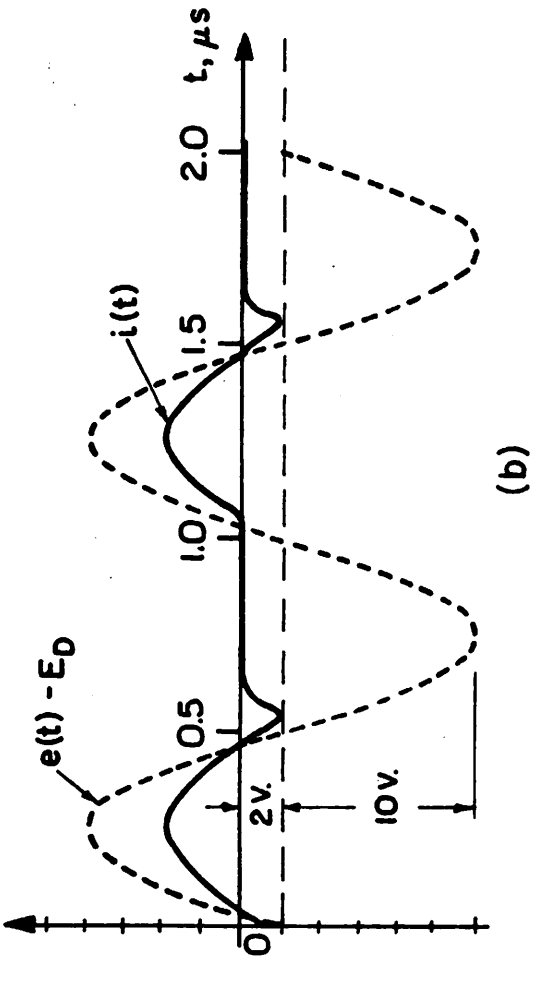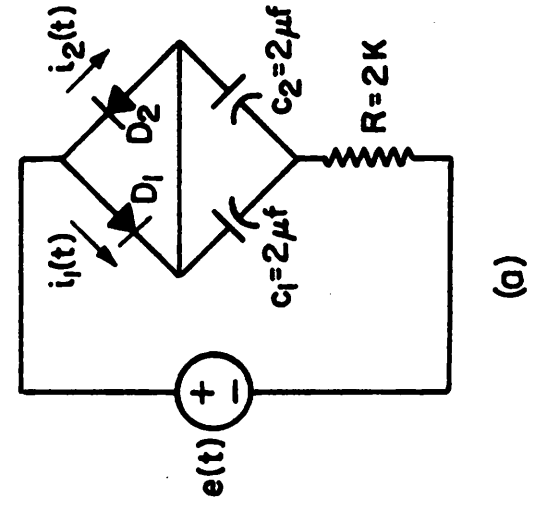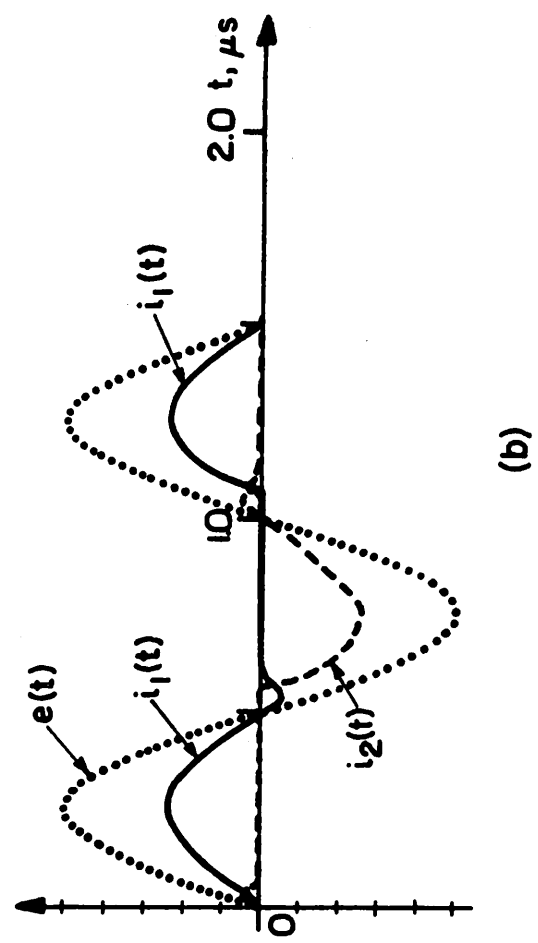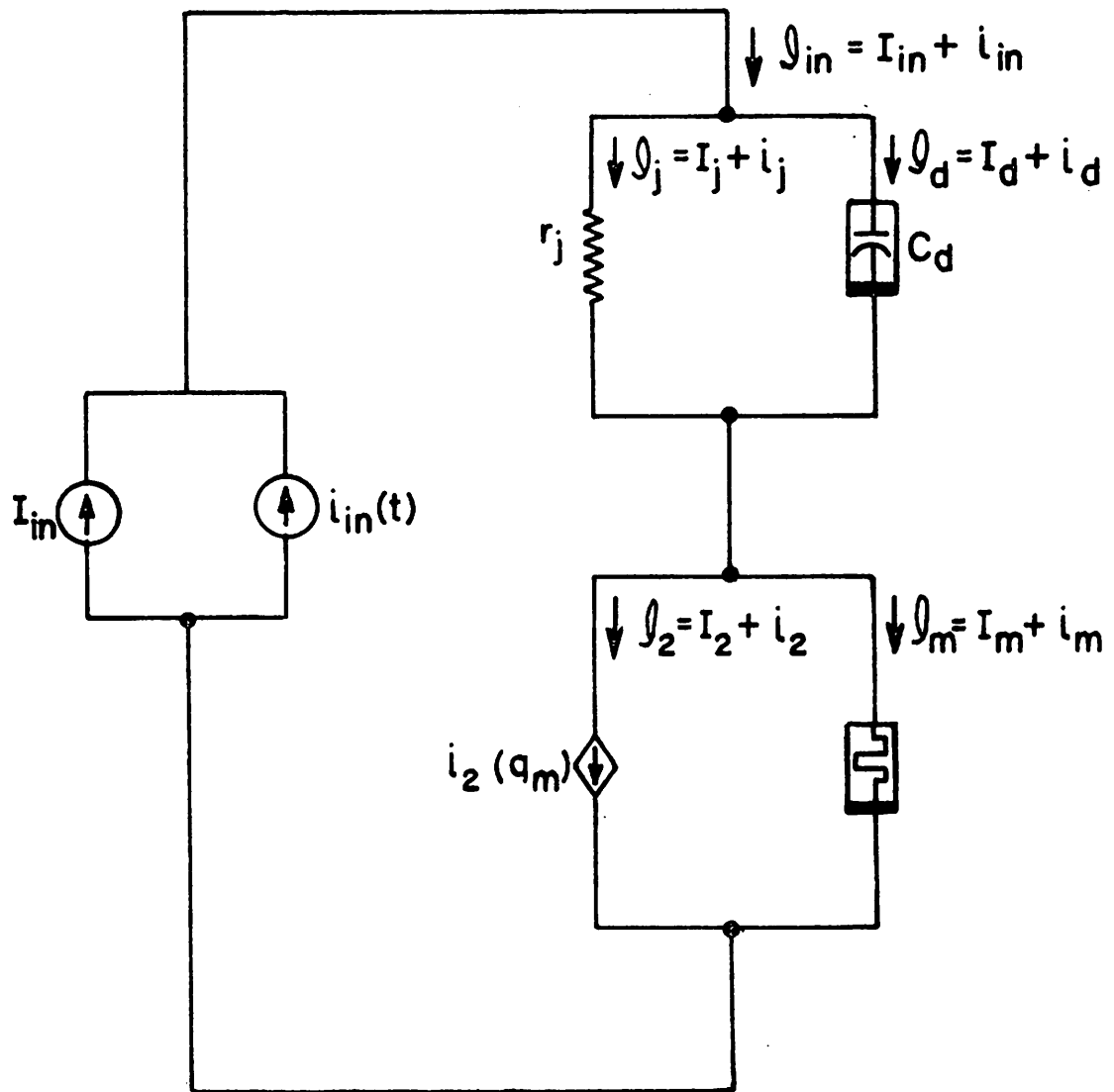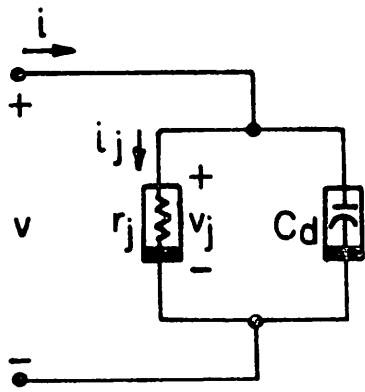$$R_m = \frac{1}{A}\int_0^{w_n}\frac{dx}{\sigma(x, q_m)}$$

Fig. 12

(a)

(b)

(c)

Fig. 13

Fig. 14

(a)

R = 2K

$i(t)$

$+$ $v(t)$ $-$

$e(t) = 10 \sin \omega t$

$E_D = 2$ volts

(b)

$i(t)$

$e(t) - E_D$

2v.

10v.

0.5   1.0   1.5   2.0 $t, \mu s$

O

Fig. 15

(a)

$i_2(t)$

D_2

$c_2 = 2\mu f$

D_1

$i_1(t)$

$c_1 = 2\mu f$

R = 2K

$e(t)$

$+$ $-$

(b)

$i_1(t)$

$e(t)$

$i_1(t)$

$i_2(t)$

1.0   2.0 $t, \mu s$

O
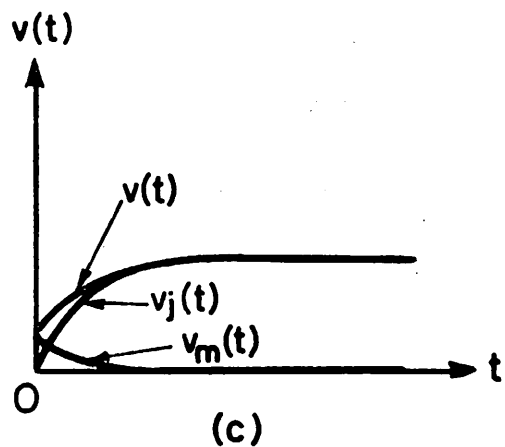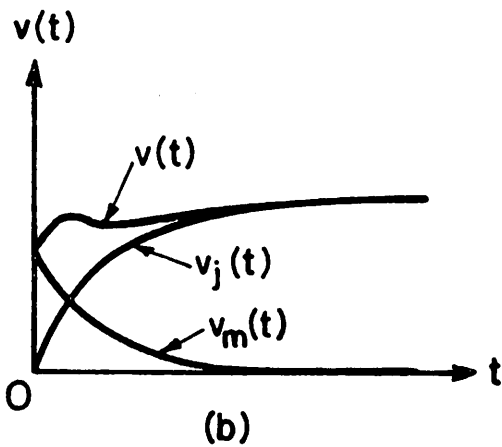
Fig. 16

$$r_j = \left(\frac{di_j}{dv_j}\right)^{-1} = \left[\frac{d}{dv_j}\left\{I_S\left[\exp\left(\frac{v_j}{V_T}\right)-1\right]\right\}\right]^{-1}$$

$$C_d = \frac{I_S\tau}{V_T}\exp\left(\frac{v_j}{V_T}\right)$$

Fig. A1

Fig. B1
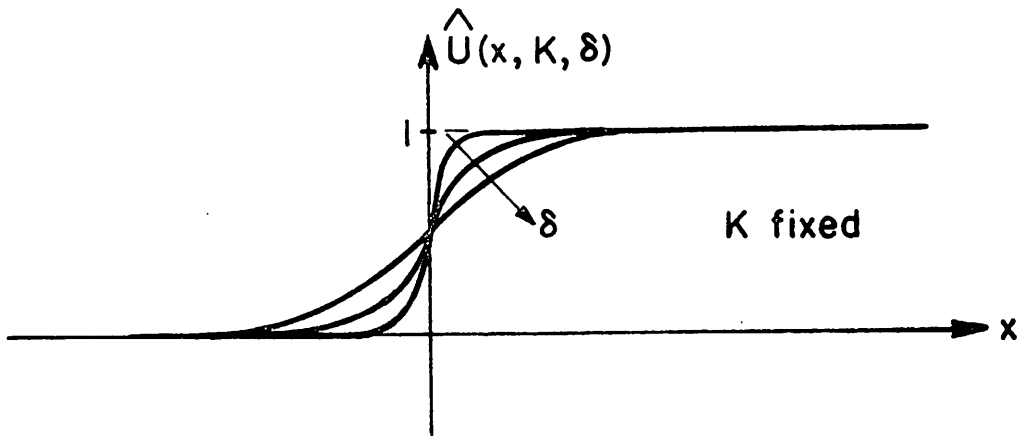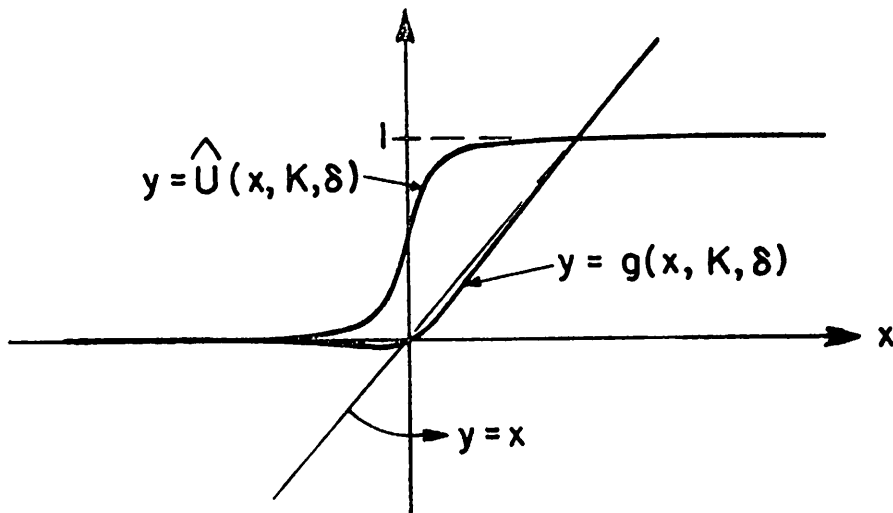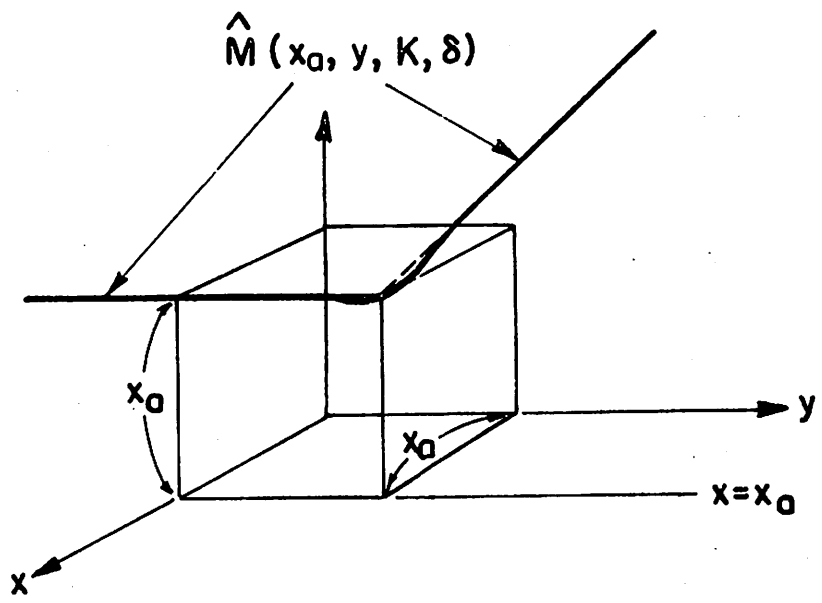

Fig. C1

$\hat{M}(x_a, y, K, \delta)$

x_a

x_a

y

$x = x_a$

x

Fig. C 2